Journal of Geochemical Exploration 179 (2017) 9–24

Contents lists available at ScienceDirect

Journal of Geochemical Exploration

journal homepage: www.elsevier.com/locate/gexplo

A new terrestrial active mineralizing hydrothermal system associated with ore-bearing travertines in Greece (northern Euboea Island and Sperchios area)

Christos Kanellopoulos[a,*], Panagiotis Mitropoulos[a], Eugenia Valsami-Jones[b,c], Panagiotis Voudouris[a]

[a] National and Kapodistrian University of Athens, Department of Geology and Geoenvironment, Panepistimioupolis Zografou, 157 84 Athens, Greece
[b] Department of Earth Sciences, Natural History Museum London, Cromwell Road, London SW7 5BD, UK
[c] School of Geography, Earth & Environmental Sciences, University of Birmingham, Edgbaston, Birmingham B15 2TT, UK

ARTICLE INFO

Keywords:
Hydrothermal system
Hot springs
Thermogenic travertine
Metallogenesis
Active terrestrial ore mineralization

ABSTRACT

The northwestern Euboea Island and the neighboring part of the mainland in eastern Central Greece, i.e. Sperchios area, contain several hot springs and active thermogenic travertine deposits, which are the surface manifestations of an active hydrothermal system, controlled by active tectonics, and supplied with heat by a 7–8 km deep magma chamber, with surface manifestation, the Plio-Pleistocene trachyandesitic volcanic center of Lichades. This hydrothermal system is fueled by a mixture of seawater and deep magmatic fluid with only limited meteoric water contribution. Thermal water samples show extreme pH, temperature and Electrical Conductivity values, with maximum values always recorded in two locations (Aedipsos and Ilia). The observed similarities in fluid compositions for most of the analyzed anions, major and trace elements, suggesting a stronger hydrothermal signature for the Northern Euboea area, perhaps reflecting greater proximity to the heat source of the hydrothermal system. The hydrothermal fluids collected and analysed were found to be highly enriched in a number of metallic and non-metallic elements e.g. up to 100 μg/L As, up to 1.1 wt.% Fe, up to 340 μg/L Ba, up to 65 μg/L Cu, up to 2.1 wt.% Cl, up to 3700 mg/L SO_4^{2-}, up to 390 μg/L Se. Some of the enrichments are reflected directly in the travertines lithogeochemistry and the metallic mineral phases found inside the travertines. A number of mineral phases including sulfides (such as pyrite, arsenopyrite, galena, chalcopyrite, sphalerite and stibnite), native elements (such as Pb and Ni), alloys (such as Au ± Cu-Ag) fluorite and REE-bearing phases (such as Ce-, Nd- and La-bearing members of hydroxylbastnäsite, cackinsite, lanthanite and sahamalite) were identified syngenetically enclosed as clastic grains within the pores of all studied travertines; the ore grade concentrations of some iron-rich travertines (up to 28.9 wt.% Fe and up to 1.83 wt.% As), as well as the high concentration of precious and base metals at the hydrothermal fluid, strongly suggest active mineralizing processes throughout the studied system. Travertines containing elevated Fe ± As and consisting of ferrihydrite in addition to aragonite/calcite, were deposited on the surface, most likely after mixing of ascending reducing hydrothermal fluids with cool seawater. The high REE content in the Fe ± As-rich travertines (up to ~465 mg/kg ΣREE) is caused by adsorption of REE-bearing phases by iron oxyhydroxides. Mineralogical and geochemical evidence (such as the presence of elements in their native form, of alloys such as Au ± Cu-Ag, the enrichment of metalloids and the abundance of REE) may indicate magmatic contribution to the hydrothermal system and accordingly to the studied travertines. We support the hypothesis that metals and metalloids were mainly derived from magmatic fluids, which successively mixed with heated-, and with oxygenated, cool seawaters at depth and on the surface respectively, resulting in the deposition of carbonate-hosted sulfide mineralization at depth, and of Fe ± As-rich travertines at the surface. The northwestern Euboea Island and Sperchios area hydrothermal system represents the first documented active terrestrial mineralizing hydrothermal system associated with ore-bearing travertines in Greece.

* Corresponding author.
E-mail addresses: ckanellopoulos@gmail.com, xkanel@geol.uoa.gr (C. Kanellopoulos), pmitrop@geol.uoa.gr (P. Mitropoulos), e.valsamijones@bham.ac.uk (E. Valsami-Jones), voudouris@geol.uoa.gr (P. Voudouris).

http://dx.doi.org/10.1016/j.gexplo.2017.05.003
Received 17 June 2016; Received in revised form 24 April 2017; Accepted 10 May 2017
Available online 12 May 2017
0375-6742/

1. Introduction

Active geothermal fields are generally recognized as modern analogues of hydrothermal ore deposits (White, 1955, 1981; Weissberg et al., 1979; Henley and Ellis, 1983; Henley, 1985). Scale deposits from geothermal energy installations have been reported to contain significant concentrations of precious and base metals, e.g. at Salton Sea - USA (McKibben et al., 1989), at Cheleken - Turkmenistan (ex-USSR, Lebedev, 1973), at Milos island - Greece (Karabelas et al., 1989), at Ohaaki, Kawerau and Rotokawa - New Zealand (Brown, 1986), at Cerro Prieto - Mexico (Mercado et al., 1989) and at Oku-Aizu - Japan (Imai et al., 1988).

Among the most impressive geothermal phenomena, the venting of hydrothermal fluids and their precipitations have been reported from several tectono-magmatic settings in both subaerial and submarine environments (e.g. Henley and Ellis, 1983, Hannington and Scott, 1988, Barnes, 1997; Dando et al., 1999, Pirajno 2009; Barnes, 2015).

In Greece, several high-, medium- and low-enthalpy geothermal fields related to the Tertiary-Quaternary magmatism and active faulting in the south Aegean active volcanic arc and the back-arc region (e.g. Jolivet et al., 2013), discharge deep hydrothermal fluids in the form of hot springs and hydrothermal vents at the surface (Gkioni-Stavropoulou, 1983; Orfanos, 1985; Sfetsos, 1988; Lambrakis and Kallergis, 2005) and shallow submarine settings (Valsami-Jones et al., 2005; Price et al., 2013; Kilias et al. 2013). Some of them are highly enriched in a number of metallic and non-metallic elements (Valsami-Jones et al., 2005; Kilias et al. 2013; Athanasoulis et al., 2009, 2016).

Northern Euboea (or Evia) and the neighboring part of the mainland in eastern Central Greece (Sperchios area) are recognized as having one of the highest geothermal gradients in Greece, after the south Aegean active volcanic arc (Fytikas and Kolios, 1979). This area is located in the periphery of the Plio-Pleistocene volcanic center of Lichades, at the western extremity of the North Anatolian Fault (Vött, 2007; Fig. 1). Some of the hot springs in this area have been known since ancient times (i.e. Aedipsos, Thermopylae). Several ancient Greek philosophers and historian (e.g. Aristotle, Thucydides and Strabo) recognized a close relationship between hot springs and earthquake activity in the area. Also, during the Atalanti's earthquake in 1894, the hot spring at Gialtra became turbid (Pertessis, 1961) and new springs appeared in the area of Aedipsos (Margomenou-Leonidopoulou, 1976).

The hot springs in this area were studied by many researchers (e.g. Minissale et al., 1989; Karagiannis et al., 1990; Gartzos and Stamatis, 1996; Mitropoulos and Kita, 1997; Gkioni-Stavropoulou, 1998; Lambrakis and Kallergis, 2005; Shimizu et al., 2005; Chatzis et al., 2008, Duriez et al., 2008; Kanellopoulos, 2006, 2011; D'Alessandro et al., 2014; Dotsika, 2015; Vakalopoulos, et al., 2016; Kanellopoulos et al. 2016b). These studies were mainly focused on the understanding of the hydrological patterns of fluid circulation, and in most cases to detect the most promising and/or less risky areas for geothermal exploration.

A salient feature of the geothermal activity in northern Euboea and neighboring part of the mainland in eastern Central Greece (Sperchios area), is the dominance of thermogenic travertine deposition from the hot springs (Kanellopoulos, 2011, 2012, 2013; Kanellopoulos et al. 2016a). Kanellopoulos (2011, 2012) reported Fe-rich varieties among the studied travertines.

Mineralized thermogenic travertines are rarely reported worldwide and are related to distinct ore deposit types (such as low- and intermediate sulfidation epithermal, Carlin-type, carbonate-replacement) and/or active geothermal systems (Bernasconi et al., 1980; Lattanzi, 1999; Daliran, 2003, 2008; Boni et al., 2007; Daliran et al., 2013; Nordstrom and Sharifi, 2014; Sillitoe, 2015; Rossi et al., 2015).

The aim of this paper is to investigate (a) the geochemistry of hydrothermal fluids from the northwestern part of Euboea Island and the neighboring part of the mainland (Sperchios area), (b) the mineralogical and geochemical composition of the newly formed thermogenic travertines of the area, and (c) to compare them with active terrestrial hydrothermal systems elsewhere, related to ore-bearing travertine deposition. Emphasis is given on their metallic and non-metallic content in an attempt to demonstrate active mineralizing processes related to a single large hydrothermal system in the area.

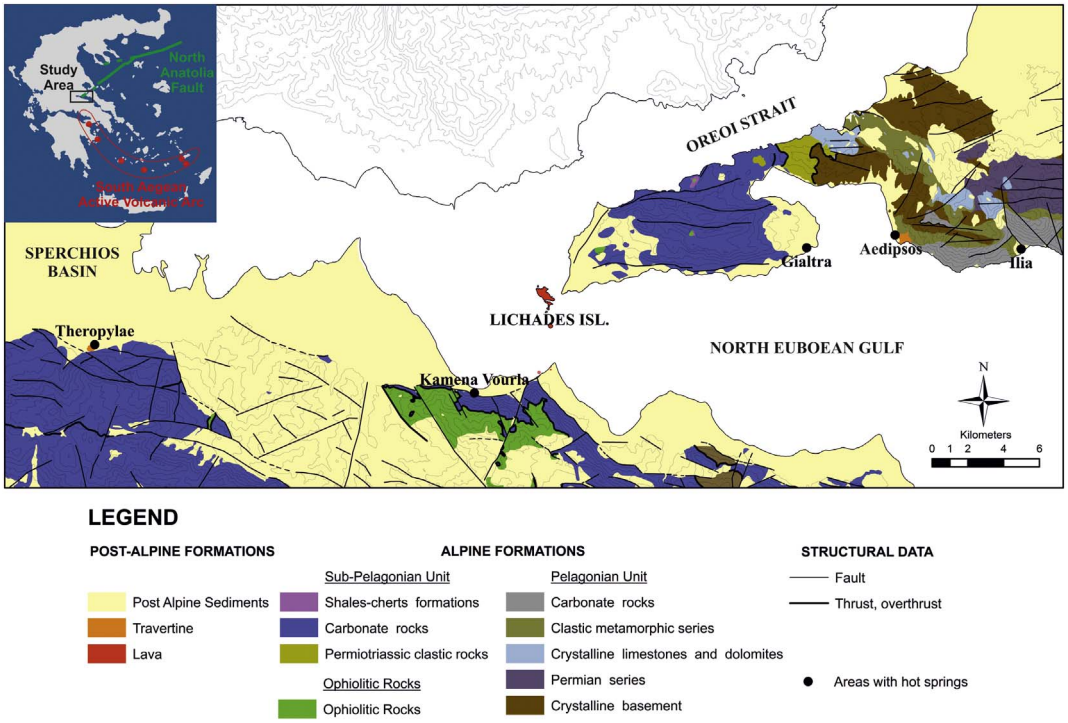

Fig. 1. Geological map showing distribution of hot spring areas in the northern Euboea Island and Sperchios area.

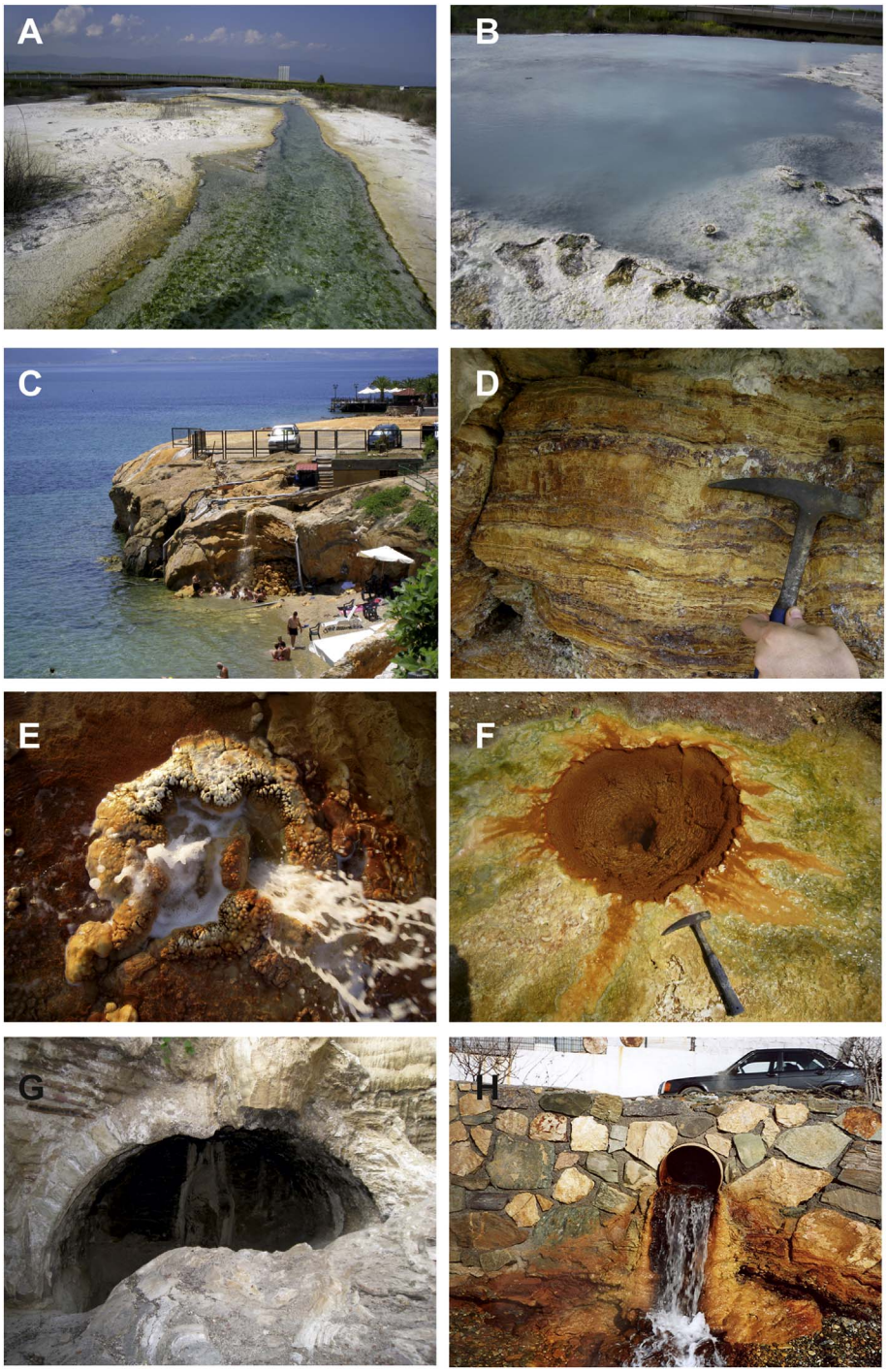

Fig. 2. Field photos demonstrating mode of occurrence of thermogenic travertine in the study areas. (A) Hot water stream depositing thermogenic travertines in Thermopylae area. (B) Hot pond at thermogenic travertines depositions in Thermopylae area. (C) Cape formation in Aedipsos, composed only by thermogenic travertine, resulting from hot water discharge into the sea. (D) Detailed photo from the cape formation (see Fig. 2C), where characteristic layers with different chemical compositions of the thermogenic travertine can be seen. (E) Self-settled artesian borehole of hot water creating a geyser at Aedipsos. (F) Artesian hot borehole, depositing thermogenic travertine in Aedipsos. (G) Ancient Roman baths, in Aedipsos, clogged by thermogenic travertine deposition. (H) A small travertine dome at Ilia, at the point of venting of the hot water from the pipe. It is a laminated Fe-rich travertine.

2. Geological setting

The study area (Fig. 1) belongs to the Pelagonian and Sub-Pelagonian geotectonic units of the Hellenides (Aubouin, 1959; Mountrakis, 1986; Jolivet et al. 2013). The eastern central part of mainland (Sperchios area) consists of Post-Alpine, Late Miocene-Pleistocene fluvio-lacustrine marls, clays, conglomerates and sands, unconformably overlying the Sub-Pelagonian Geotectonic Unit. The latter, is made up from bottom to top of a basement of carbonate rocks (limestones and dolomites) of Middle Triassic-Middle Jurassic age, and an ophiolitic thrust sheet that is a relic of the Tethyan oceanic crust (Celet, 1962; Orfanos and Sfetsos, 1975; Kranis, 1999, 2007). The Thermopylae and Kamena Vourla hot springs mainly discharge from the carbonate rocks of Middle Triassic-Middle Jurassic age.

The northern Euboea, where the hot springs at Aedipsos (or Aidipsos or Edipsos), Ilia and Gialtra occur, consists of both Pelagonian and Sub-Pelagonian Geotectonic Units (Fig. 1). In the studied area, a lower series, with a Permian–Triassic volcaniclastic

complex overlie a pre-middle to middle Carboniferous metamorphic basement and is overlain by middle Triassic shallow marine clastic and carbonate rocks intercalated with volcanic rocks best developed at the southeast part of Aedipsos (Katsikatsos et al., 1984). This sequence is overlain by Jurassic limestones and Late Jurassic–Early Cretaceous ophiolites (Katsikatsos et al., 1984; Scherreiks, 2000). The Paleozoic and Mesozoic sequences are folded or imbricated as the result of two main tectonic events (Alpine and Eo-Alpine). In the greater area of Northern Euboea lignite layers have been identified inside Neogene-Lower Pleistocene lake sediments (Vakalopoulos et al., 2000). The hot springs mainly discharge from the metamorphic basement rocks. In the case of Aedipsos the hot springs are venting through thermogenic travertines, which are deposited on top of the basement metamorphic rocks. In the case of Gialtra the hot springs are discharge from Neogene-Quaternary deposits, which are deposited on top of the basement carbonate rocks.

The study area is located at the intersection between a series of ENE-WSW faults of the Euboea-Sperchios rift and the NE-SW faults system of the Oreoi Strait, at the western extremity of the North Anatolian Fault (McKenzie, 1970, 1972; Shaw and Jackson, 2010). The study area is one of the most neotectonically active areas in Greece dominated by extensional tectonics similarly to the rest of the Aegean Sea. Oreoi Strait is a narrow symmetrical NE-SW graben. The Northern Euboea Gulf is part of the 130-km long Euboea-Sperchios rift, which trends ESE-WNW and currently extends at a rate of 1–2 mm/yr (Clarke et al., 1998). Its western part (Sperchios) is controlled by north-throwing E-W to ESE-WNW range-bounding normal faults, which extend into its eastern part (Northern Euboean Gulf), where a polarity change is observed, with SE-NW, E-W and ENE-WSW, mainly offshore faults which mark the northern boundary of the Gulf and uplifts North Euboea (Sakellariou et al., 2007). The study area is highly faulted due to extensional tectonics and it is characterized by E-W to ENE-WSW, NNE-SSW to NE-SW and SE-NW fault systems (Angelopoulos et al., 1991; Tzitziras and Ilias, 1996; Vavassis, 2001; Kranis, 1999, 2007; Palyvos et al., 2006).

The central part of the investigated area is occupied by the Plio-Pleistocene volcanic center of Lichades islands (Georgalas, 1938; Georgiades, 1958; Pe-Piper and Piper, 2002), made of 0.5 Ma old (K-Ar, Fytikas et al., 1976) trachyandesite lava flows. Trachyandesite lavas at the nearby Kamena Vourla were dated at 1.7 Ma (K-Ar, Bellon et al., 1979). Magma emplacement took place along the major tectonic structures in the area (Kranis, 1999).

Innocenti et al. (2010), based on Sr–Nd–Pb isotopic data, related this volcanic activity with the large volcanic belt that developed north of the Pelagonian–Attic–Cycladic–Menderes massifs, encompassing a 35 Ma timespan which is widespread over a large area from NW Greece–Macedonia to the Aegean–western Anatolia. According to the above authors, the Euboea-Kamena Vourla volcanic products are orogenic in character and partially contemporaneous with the south Aegean active volcanic arc, but with different geochemical features, related to distinct magma sources (e.g. lithospheric mantle wedge and a depleted asthenospheric mantle wedge north and south of the Pelagonian–Attic–Cycladic–Menderes massifs respectively).

Karastathis et al. (2011) showed that there is a magma chamber at depths below 8 km under the North Euboean Gulf area, using low seismic P-wave velocity values and high Poisson ratios, also coincident with a Curie surface estimated at 7–8 km depth.

3. Locations of major hot spring areas and thermogenic travertine areas

Five major areas with hot spring activity occur around the volcanic center of Lichades islands (Fig. 1 and 2; Table 1), which were studied in the period 2004–2008. Three of them are located in the northwestern part of Euboea Island (Aedipsos, Ilia, Gialtra; Fig. 2) and two are in the neighboring part of the mainland in eastern Central Greece (Sperchios area: Kamena Vourla, Thermopylae; Fig. 2). A common feature of these hot springs is the deposition of several morphological types and lithotypes of thermogenic travertine as the hot waters cool, degas and rapidly precipitate calcium carbonate (Kanellopoulos, 2012, 2013).

Although the formation of these thermogenic travertines is dominantly controlled by abiotic factors, also biotic factors are proposed to be contributing (Kanellopoulos, 2014b; Kanellopoulos et al., 2016a).

The major hot springs in the area and their geochemical characteristics, in summary, are as follows:

i) Aedipsos (or Edipsos or Aidipsos) includes hot springs with temperatures ranging from 50.8 to about 82 °C, pH from 5.6 to 7.5 and degassing mainly H_2S and CO_2 (D'Alessandro et al., 2014). In several cases, artesian boreholes present vigorous bubbling, indicating high gas pressure at depth. Large deposits of newly formed and fossil thermogenic travertine are characterized by a great variety of macro- and micro- facies (Kanellopoulos, 2012, 2013) and colors varying from white-yellow to red, with orange prevailing.

ii) At the Ilia area, there is only one hot spring/artesian borehole, located near the seashore, with a temperature ranging from 61 to 63 °C, pH from 6.1 to 6.4 and degassing mainly CO_2 (D'Alessandro et al., 2014). The travertine at Ilia covers a small area (few square meters) and has a reddish-brown color.

iii) At the Gialtra area a twin hot spring with temperature in the range from 43 to 43.5 °C, pH from 6.4 to 6.5, degassing mainly N_2 (D'Alessandro et al., 2014) and low discharge is located near the seashore. In the area, no significant travertine formation has identified.

iv) At Kamena Vourla several hot springs occur, with temperatures, ranging from 29.6 to 35.5 °C, pH from 5.9 to 6.2 and degassing mainly N_2 (D'Alessandro et al., 2014). In the area, no significant travertine formation has identified.

v) The Thermopylae hot springs have similar temperatures and pH values to those at Kamena Vourla, ranging from 32.8 to 33.5 °C and from 6 to 6.2 respectively, but degassing mainly CO_2 (D'Alessandro et al., 2014). In Thermopylae, extensive deposits of newly formed and fossil thermogenic travertine occur (Kanellopoulos, 2012, 2013). Their color varies from white to gray.

4. Materials and methods

4.1. Hot water samples

A total of 28 hydrothermal fluid samples from hot springs and boreholes used in most cases for thermal spa/bathing therapies were collected and analyzed (Table 1). The water samples were collected in four sampling campaigns in 2004, 2005, 2007 and 2008. Selected hot springs were sampled from different time periods (dry and wet hydrological periods), in order to assess possible variation of their chemical content with time.

Unstable physicochemical parameters such as temperature, pH, Electrical Conductivity (E.C.) and Total Dissolved Solids (T.D.S.) were measured in-situ (Table 1), using portable scientific equipment of the Laboratory of Economic Geology and Geochemistry, National and Kapodistrian University of Athens. The pH-meter was calibrated with standard buffer solutions of pH 4.0 and 7.0 before measuring the first sample each day. The pH measurement error, including accuracy and reproducibility, is better than ± 0.05 pH units. Temperature was measured with the probe connected to the pH-meter and the error is estimated to be less than ± 0.3 °C.

From each sampling site, samples were collected in a 1 L and 100 mL polyethylene bottles for laboratory analyses. The smaller aliquot intended for the determination of metals were filtered through 0.45 μm membrane filters and acidified down to pH < 2 with analytical grade HNO_3 (Suprapur 65%). The samples were stored in a portable cooler containing ice packs, transported to the laboratory and refrigerated at 4 °C until analysis. The 1 L polyethylene bottles used for major ion determinations were filtered upon arrival at the laboratory but not acidified. Nitrate ions were measured by the cadmium

Table 1
Physiochemical parameters, hydrochemical type and chemical analysis of the studied hot waters conducted by Spectrophotometer and titration.

Sample no.	Locality	T (°C)	pH	T.D.S. (g/L)	E.C. (mS/cm)	PO_4^{3-} (mg/L)	NO_3^- (mg/L)	SO_4^{2-} (mg/L)	Cl^- (mg/L)	HCO_3^- (mg/L)	Hydroc. type	Description of samp. site
GIA-4	Gialtra	43.4	6.46	26.68	55.12	0.1	4.4	3700	16,300	220	Na-Cl	Spring
GIA-11 (GIA-4)[a]	Gialtra	43	6.43	26.16	52.38	0.289	3.6	3400	18,470	228	Na-Cl	Spring
AD-1	Aedipsos	80.5	6.43	54.52	27.12	0.12	7.0	1500	16,130	558	Na-Cl	Borehole
AD-20 (AD-1)[a]	Aedipsos	82	7.4	26.98	56.73	0.33	6.2	1400	21,120	352	Na-Cl	Borehole
AD-2	Aedipsos	75	5.85	53.64	26.68	0.08	6.6	1600	17,300	518	Na-Cl	Borehole
AD-21 (AD-2)[a]	Aedipsos	74	7.15	24.54	53.28	0.15	5.3	1300	19,360	568	Na-Cl	Borehole
AD-3	Aedipsos	60.7	5.65	24.52	24.44	0.24	7.9	1600	13,300	534	Na-Cl	Borehole
AD-4	Aedipsos	65.4	6.86	41.8	20.76	0.17	7.0	1100	13,900	520	Na-Cl	Spring
AD-5	Aedipsos	69.9	6.3	52.96	26.24	0.17	7.0	1200	14,900	590	Na-Cl	Borehole
AD-6	Aedipsos	50.8	7.54	54.68	27.2	0.16	5.7	1400	16,000	296	Na-Cl	Spring
AD-15	Aedipsos	55.6	7.35	27.2	54.64	0.35	8.4	1500	18,000	456	Na-Cl	Borehole
AD-100	Aedipsos	70.5	6.52	26.61	53.31	0.63	4.2	1200	18,900	480	Na-Cl	Borehole
AD-101	Aedipsos	61	6.34	28.26	56.58	0.36	4.5	400	17,540	480	Na-Cl	Borehole
AD-102	Aedipsos	74	6.4	26.25	52.56	0.28	5.7	1800	19,230	510	Na-Cl	Borehole
AD-103	Aedipsos	73.3	6.4	26.49	53.07	0.52	14.4	1200	17,410	528	Na-Cl	Borehole
AD-104	Aedipsos	70	6.15	25.71	51.48	0.19	3.6	2000	17,930	548	Na-Cl	Borehole
AD-105	Aedipsos	58	7.13	24.54	49.17	0.54	5.4	1600	16,160	315	Na-Cl	Borehole
HL-1	Ilia	60.9	6.07	9.3	18.5	0.51	11.9	744	12,400	480	Na-Cl	Spring
AD-9 (HL-1)[a]	Ilia	63.4	6.25	18.8	37.72	0.62	11.4	800	12,700	554	Na-Cl	Spring
HL-11(HL-1)[a]	Ilia	63	6.45	24.75	49.56	0.31	12	700	12,050	424	Na-Cl	Spring
THE-1(KB-5)[a]	Thermopylae	40.4	5.95	7.55	15.13	0.29	12.8	510	4400	756	Na-Cl	Spring
KB-5	Thermopylae	33.5	5.97	5.55	11.85	0.22	4.0	440	1800	803	Na-Cl	Spring
KBE-10	Kam. Vourla	32.8	6.24	22.54	11.3	0.84	0.7	744	6720	540	Na-Cl	Borehole
KB-1	Kam. Vourla	35.5	5.92	11.53	16.6	0.06	4.0	960	7250	567	Na-Cl	Spring
KB-3A	Kam. Vourla	29.6	6.19	8.14	16.31	0.09	3.7	580	4650	560	Na-Cl	Spring
KB-3B	Kam. Vourla	30.2	6.09	7.96	15.92	0.19	4.0	560	4900	524	Na-Cl	Spring
KB-3C	Kam. Vourla	30.3	6.14	8.23	16.5	0.1	4.0	580	5000	576	Na-Cl	Spring
KB-4	Kam. Vourla	30.3	6.06	9	18.13	0.15	3.1	680	5500	650	Na-Cl	Spring

[a] In parenthesis are the codes for those samples which were measured again in a different time period.

reduction method [see 4500-NO_3 E, Clesceri et al., 1989], SO_4^{2-} by the turbidimetric method [see 4500-SO_4 E, Clesceri et al., 1989] and Cl^- by the mercuric nitrate method [see 4500-Cl C, Clesceri et al., 1989] using a Hach DR/2000 or DR/4000 spectrophotometer. Alkalinity (as HCO_3^-) was measured using the titration method [see 2320-B, Clesceri et al., 1989]. The concentrations of K^+ and Na^+ were determined by flame emission photometry (Jenway, PFP 7, see 3500-K B and 3500-Na B, Clesceri et al., 1989). Calcium ions and Mg^{2+} were determined by flame atomic absorption spectroscopy (see 3500-Ca and 3500-Mg, Clesceri et al., 1989) using a Perkin Elmer 603 instrument and trace metal elements by graphite furnace atomic absorption spectroscopy (Perkin Elmer 1100B).

Elements Cd, Co, Cr, Mn, Pb, Ni, Fe, Zn were determined by Atomic Absorption Spectrometry (AAS, Perkin Elmer 1100B), with Graphite Furnace (HGA-400). When concentrations were high (> 0.1 mg/L), Flame Atomic Absorption Spectrometry (F-AAS) was used instead for these elements (Table 2). Multi-element standard solutions prepared by serial dilution of single certified standards were used for calibration of analytical instruments. These parts of the chemical analyses were performed at the Laboratories of the Faculty of Geology and Geoenvironment, National and Kapodistrian University of Athens, according to the Standard Methods for the Examination of Water and Wastewater (Clesceri et al., 1989). Furthermore, selected samples were analyzed by Inductively Coupled Plasma–Atomic Emission Spectroscopy (ICP-AES) and by Inductively Coupled Plasma-Mass Spectrometry (ICP-MS) for a large group of elements at the Natural History Museum of London or at the ACME Analytical Laboratories Ltd., Canada (Table 3). Analytical data quality was assured by use of certified reference material samples in randomized positions within the analytical batch and by blank and duplicate analysis of a proportion of the samples.

4.2. Travertine samples

The mineralogical composition of the main mineral phases in travertines was identified mainly by X-ray Diffraction, at the Department of Geology and Geoenvironment, National and Kapodistrian University of Athens. XRD analysis was carried out using a Siemens Model 5005 X-ray diffractometer, Cu Ka radiation at 40 kV, 40 nA, 0.020° step size and 1.0 s step time. The XRD patterns were evaluated using the EVA 10.0 program of the Siemens DIFFRACplus and the D5005 software package. Minor mineral phases were identified by Scanning Electron Microscopy and Energy Dispersive Spectroscopy (EDS). SEM-EDS analyses was carried out using a Jeol JSM 5600 SEM instrument, equipped with an Oxford ISIS 300 micro analytical device, at the Department of Geology and Geoenvironment, National and Kapodistrian University of Athens. Selected samples were analyzed at the Natural History Museum of London with a JEOL 5900LV, equipped with an Energy Dispersive X-ray (EDX) and a Wavelength Dispersive X-ray (WDX).

The travertine samples were analyzed for whole rock chemical composition after drying and pulverizing in an agate mortar and mill to < 0.075 mm. The samples were digested with HNO_3 and analyzed by Inductively Coupled Plasma–Atomic Emission Spectroscopy method (ICP-AES, Vista-PRO Simultaneous) for Ca, Na, P, S, Si and by Inductively Coupled Plasma-Mass Spectrometry method (ICP-MS, Varian) for 36 trace elements (inc. REE) at Natural History Museum of London (Table 6). Analytical data quality was assured by introduction of internal standards, use of certified and house reference material samples in randomized positions within the analytical batch and by blank and duplicate analysis of a proportion of the samples (Ramsey et al., 1987). Analytical bias and precision were subsequently calculated and found to be within acceptable limits.

5. Results

5.1. Hot springs

5.1.1. Geochemistry of hydrothermal fluids

Temperatures of the hydrothermal fluids vary from 43 to 82 °C in the hot springs of North Euboea Island and from 30 to 40.6 °C in those

Table 2
Chemical analysis of the studied hydrothermal fluids conducted by AAS and flame photometer.

Area	Sample no.	Cd (μg/L)	Co (μg/L)	Cr (μg/L)	Mn (μg/L)	Pb (μg/L)	Ni (μg/L)	Fe (μg/L)	Zn (μg/L)	Na (mg/L)	K (mg/L)	Ca (mg/L)	Mg (mg/L)
Euboea	GIA-4	1	bdl	bdl	16	3	bdl	310	5	12,000	310	1090	540
	AD-1	1	bdl	bdl	17	4	bdl	270	3	10,600	350	1140	301
	AD-2	1	bdl	bdl	30	4	bdl	900	8	10,400	340	1110	299
	AD-3	1	bdl	bdl	20	3	bdl	170	7	9600	310	1070	262
	AD-4	1	bdl	bdl	130	3	bdl	90	7	8400	270	910	218
	AD-5	1	bdl	bdl	60	6	bdl	1180	4	9600	270	1140	291
	AD-6	1	bdl	bdl	21	5	bdl	160	15	10,200	330	1040	297
	AD-15	1	250	bdl	22	1	bdl	190	8	10,500	340	1090	295
	AD-20	bdl	bdl	bdl	55	1	bdl	150	3	9900	280	1210	343
	AD-21	bdl	bdl	bdl	43	1	bdl	1200	2	9100	290	1170	340
	HL-1	bdl	4	12	490	4	bdl	4900	13	6900	210	1070	237
	AD-9	bdl	bdl	17	430	2	bdl	11,000	6	7300	220	1060	219
Eastern Central Greece	THE-1	1	1	0.3	1	3	3	5	4	2750	75	470	219
	KB-5	0.1	3	bdl	2	2	2	29	9	3400	90	520	215
	KBE-10	bdl	6	3	780	4	35	1040	8	3800	83	510	267
	KB-1	0.2	9	bdl	1490	2	37	290	8	5900	166	720	323
	KB-3A	0.2	1	bdl	8	2	6	26	13	4200	86	520	220
	KB-3B	0.1	3	bdl	7	2	6	23	11	3800	91	480	197
	KB-3C	0.2	2	bdl	7	2	6	38	12	4000	88	520	218
	KB-4	0.2	bdl	bdl	2	3	8	100	8	5000	132	650	291

bdl = below detection limit.

of Sperchios area (Table 1). The highest temperatures were recorded in Aedipsos area (82 °C). The temperature of each individual hot spring remained relatively constant over the period of sampling.

Some samples have pH values near 7 (neutral; Table 1), however in most cases the studied hydrothermal fluids were characterized by slightly acidic pH. The lowest pH values (< 5.5) were measured in hot springs from Sperchios area and the highest values in the Aedipsos samples (max. 7.5).

Total Dissolved Solids (T.D.S.) and Electrical Conductivity (E.C.) in Euboea samples varies from 18 to 54 g/L and from 37 to 56 mS/cm respectively, with maximum values at Aedipsos samples (Table 1) and lower values (7–11 g/L, 18–15 mS/cm resp.) at samples from Sperchios area.

Cl^- is the dominant anion in all analyzed solutions (up to 2.2 wt% Cl). It varies from 1.2 to 2.2 wt% Cl in Euboea samples and from 1800 to 7250 mg/L in those from Sperchios area. The Euboea samples show concentrations closest to seawater (3.5 wt% Cl). The studied samples show enrichment in B (up to 10.7 mg/L), Sr (up to 30 mg/L) and Li (up to 1.5 mg/L) in comparison with seawater (4.6 mg/L B, 8 mg/L Sr; and 0.17 mg/L Li; Goldberg, 1963).

Concentrations of Na^+, K^+, Ca^{2+}, SO_4^{2-}, Cl^- show co-variation (Fig. 3), suggesting common source. Maxima (12,000 mg/L, 360 mg/L,

Table 3
Chemical analysis of hydrothermal fluids conducted by ICP-AES and ICP-MS.

		Northern Euboea											Eastern Central Greece		
		Aedipsos								Gialtra	Ilia		Thermopylae	Kamena Vourla	
		AD-1[a]	AD-5[a]	AD-100	AD-101	AD-102	AD-103	AD-104	AD-105	GIA-11	HL-1[a]	HL-11	THE-1[a]	KBE-10[a]	KB-1[a]
Ag	(μg/L)	10	7	–	–	–	–	–	–	–	bdl	–	bdl	1.1	0.6
Al	(μg/L)	bdl	370	bdl	bdl	bdl	bdl	bdl	bdl	bdl	218	bdl	16	17	bdl
As	(μg/L)	69	67	bdl	bdl	bdl	bdl	bdl	bdl	bdl	84	bdl	100	28	30
Au	(μg/L)	bdl	bdl	–	–	–	–	–	–	–	bdl	–	bdl	bdl	bdl
B	(mg/L)	9.8	9.1	–	–	–	–	–	–	–	10.7	–	2.9	3.5	3.3
Ba	(μg/L)	340	280	160	160	160	160	130	120	40	270	120	130	150	190
Be	(μg/L)	–	–	0.6	0.5	0.6	0.6	0.6	bdl	bdl	–	0.6	–	–	–
Br	(mg/L)	67.5	66.4	–	–	–	–	–	–	–	4.4		14.7	24.6	25.1
Cs	(μg/L)	390	410	290	300	290	290	280	200	90	460	320	260	190	200
Cu	(μg/L)	54	65	8	9	9	10	8	16	15	54	6	15	20	23
Ga	(μg/L)	–	–	1	1.1	1.3	1.1	1.2	1	–	–	0.6	–	–	–
Ge	(μg/L)	bdl	bdl	11	11	11	11	10	9	17	8	12	1	bdl	bdl
La	(μg/L)	1.6	1.6	bdl	bdl	bdl	bdl	bdl	bdl	bdl	1.9	bdl	0.2	0.2	0.2
Li	(μg/L)	1520	1450	1410	1420	1430	1460	1390	1290	620	300	bdl	890	390	360
Rb	(μg/L)	292	290	270	270	270	270	260	230	161	350	310	270	120	130
Sb	(μg/L)	bdl	bdl	bdl	bdl	bdl	bdl	1	bdl	bdl	bdl	bdl	bdl	bdl	bdl
Se	(μg/L)	380	390	–	–	–	–	–	–	–	270	–	89	140	150
Si	(mg/L)	37	35	21	21	21	22	21	20	8.6	69	43	18	27	15
Sn	(μg/L)	bdl	bdl	bdl	bdl	bdl	bdl	bdl	bdl	bdl	bdl	bdl	bdl	bdl	2.3
Sr	(mg/L)	17	17	8.2	8.5	8.5	8.6	8.4	7.9	7.9	30	26	12	5.8	6.1
Tl	(μg/L)	1.9	2.2	3	2	3	3	2	2	bdl	1.64	2	bdl	0.3	0.4
U	(μg/L)	bdl	bdl	bdl	bdl	bdl	bdl	bdl	1	9	bdl	0	bdl	12	10
V	(μg/L)	76	70	25	26	26	28	26	26	28	50	18	20	28	30
Y	(μg/L)	bdl	bdl	0.07	0.07	0.07	0.07	0.2	0.08	0.07	bdl	0.13	0.2	0.2	0.2

bdl = below detection limit.
[a] Analysis made in ACME labs, the rest of the samples analyzed in NHM labs.

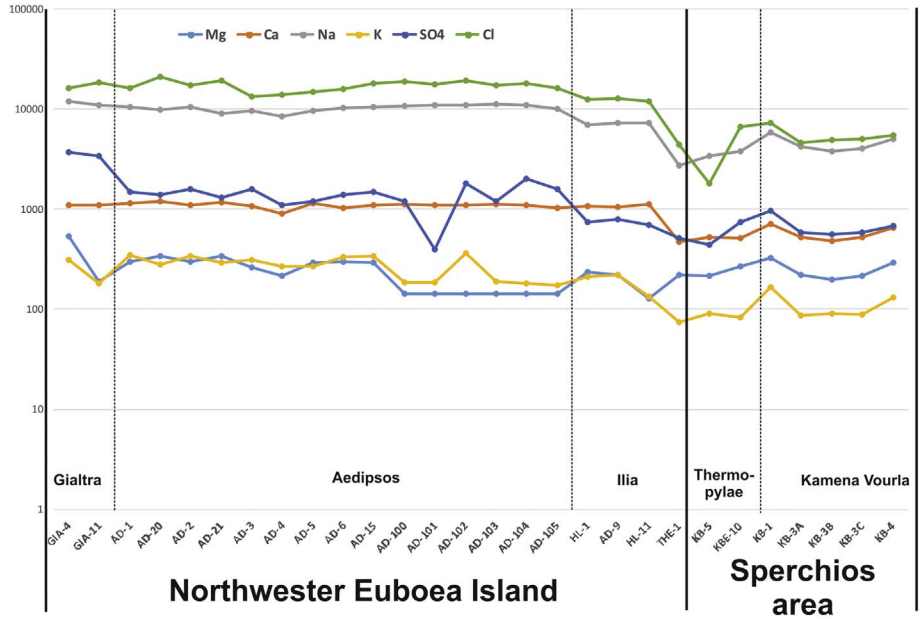

Fig. 3. Logarithmic diagram presenting the concentrations (in mg/L) of selected major and trace ions in the studied hydrothermal fluids. A co-variation between Na, K, Mg, Ca, SO_4 and Cl can be observed.

1210 mg/L, 3700 mg/L, 21,100 mg/L respectively) occur in Euboea samples (Fig. 3). The average concentration of Ca in Euboea samples is 1095 mg/L and in Sperchios area is 550 mg/L.

In order to evaluate the hydrochemistry of the studied hydrothermal fluids the chemical analyses were plotted in Piper diagrams, where all samples display the same hydrochemical type i.e. Na-Cl (Fig. 4). Based on the Cl-SO_4-HCO_3 diagram (Fig. 5A) all samples were characterized as near neutral chloride waters, as chloride is the prevalent ion. The very limited distribution of the studied samples on the characterization diagrams reflect chemical relation among them. Finally, all samples plot in the field of mature waters on the Na/1000-√Mg-K/100 diagram (Fig. 5B). The Sperchios samples plot near the boundary between mature-immature waters and are under partial chemical water-rock equilibrium, while the Euboea samples plot much closer to a full equilibrium.

Most trace elements, present their maxima in the Euboea samples and more specifically in the Aedipsos hot springs (e.g. up to: 10 μg/L Ag; 340 μg/L Ba; 67.5 mg/L Br; 20 μg/L Cr; 65 μg/L Cu; 76 μg/L V; Tables 2 and 3). Some trace elements like Fe (up to 11,000 μg/L), Cs (up to 460 μg/L), Ge (12 μg/L), show their maxima in the Ilia samples (Table 2). Only few trace elements, for example Co and Ni, show their maxima in the Sperchios area samples, where the highest concentrations were detected in Kamena Vourla (Table 2). The high correlation coefficient of 0.84 between Co and Ni suggests a common source (Table 2). The Kamena Vourla samples display the highest U content among all the studied material (up to 12.5 μg/L; Table 3). This is in

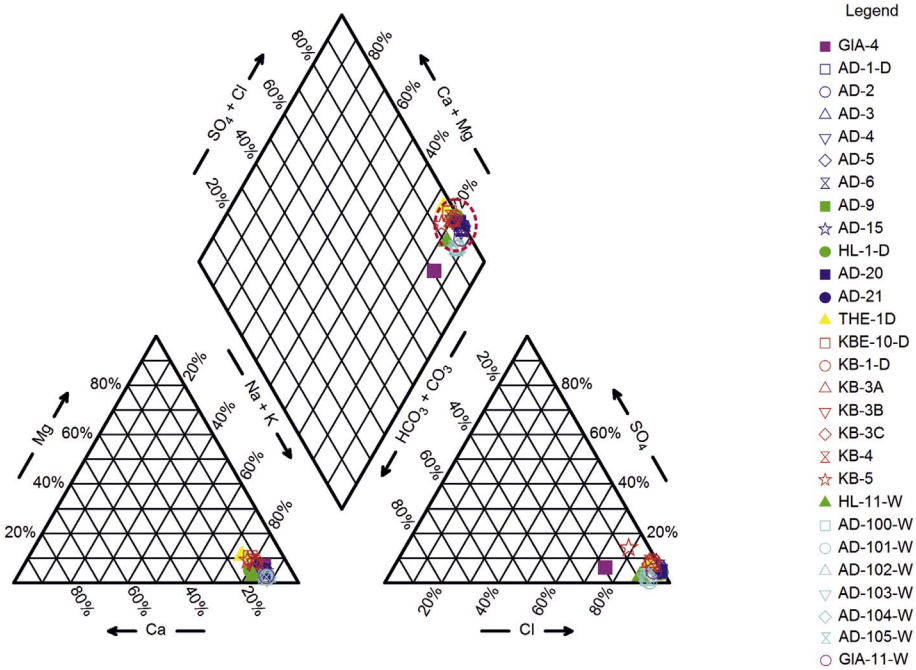

Fig. 4. Chemical composition of hydrothermal fluid samples plotted in the Piper trilinear diagram (red cycle: plotting area of the south Aegean active volcanic arc hydrothermal fluids, after Fytikas and Andritsos, 2004). (For interpretation of the references to color in this figure legend, the reader is referred to the web version of this article.)

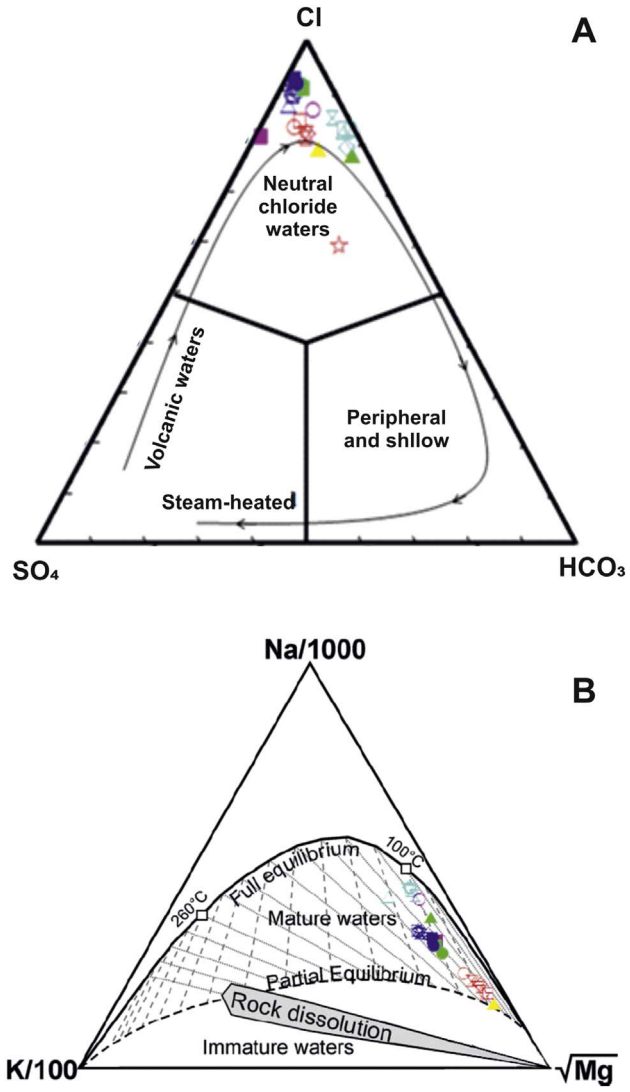

Fig. 5. Chemical composition of hydrothermal fluid samples plotted in (A) Cl-SO_4-HCO_3 trilinear diagram (Diagram after Giggenbach, 1997) and (B) Na/1000–√Mg-K/100 trilinear diagram (diagram after Giggenbach, 1988. The symbiology of the samples is the same with Fig. 4).

accordance to uranium enrichment in the cold groundwater of the same area, considered to be the result of U leaching from underground bedrock (Kanellopoulos, 2006). In all Euboea samples, except one sample from Gialtra (GIA-11) and one from Aedipsos (AD-105), the U content was below the detection limit.

Zn and Pb show low concentrations (up to 15 μg/L Zn and 6 μg/L Pb) with small variations and they are present in all samples (Tables 2 and 3). The concentration of Pb and Zn in Euboea ranges from 1 to 6 mg/L and 3–15 μg/L and in Sperchios area from 2 to 4 mg/L and 4–13 μg/L, respectively.

Sampling at different seasons indicated no significant change of the composition of the hydrothermal fluid (Tables 2). However, there is a small trend to lower concentrations during the rainy period and this may indicate a dilution of the dissolved elements after mixing between hydrothermal fluids and meteoric water.

5.2. Thermogenic travertines

5.2.1. Mineralogy

The main mineral phases of the travertines are calcite coexisting with aragonite. At Aedipsos the predominant phase is either aragonite or calcite. At Thermopylae only calcite was identified as the predominant mineral phase within the travertines. The chemical composition of calcium carbonate mineral phases varies from area to area in terms of trace elements (Kanellopoulos, 2012). The Ilia travertine is mainly composed of aragonite/calcite and a poorly crystalline hydrous ferric oxyhydroxide phase, which was identified as ferrihydrite by XRD analysis (Fig. 6), in accordance to Kanellopoulos (2012). The Ilia travertine shows usually a lamination lithotype creating botryoidal shapes (Kanellopoulos, 2012). In hand specimens two different bands can be distinguished: (a) a reddish brown band with a lustrous metallic sheen (Fe-rich) and (b) a light brown band (Ca-rich i.e. aragonite/calcite; Fig. 7A, B). Selected samples from each band were analyzed by XRD, in order to verify their main mineral phases and they were thoroughly studied using Scanning Electron Microscope (SEM). A magnified view of the iron-rich band shows finer scale laminae of hydrous ferric oxyhydroxide phase alternating with aragonite-rich laminae at intervals of a few tens of micrometers (up to 100 μm, Fig. 7C). The aragonite-rich parts contain 32–35 wt% Ca, 1–6 wt% Fe, 0.5–1 wt% Si and 0–1 wt% As, while the Fe-rich parts display a significant reduction in Ca content (2–3 wt%) and an increase of Fe, Si and As contents (38–39 wt%, 5–7 wt% and 2–4 wt% respectively; see also Fig. 7C, D).

Most of the samples contain also minor amounts of metallic and non-metallic mineral phases. The most common non-metallic phases were gypsum, halite, barite, fluorite and REE bearing phases (Ce-, Nd- and La-bearing members of hydroxylbastnäsite, cackinsite, lanthanite and sahamalite). In the Aedipsos samples, halite crystals were developed at the rims of the pores of travertine, as a result of the high Cl and Na concentrations of the hydrothermal fluid and the evaporation processes. Metallic mineral phases include pyrite, As-rich pyrite, arsenopyrite, stibnite, galena, Fe-rich sphalerite, chalcopyrite, native elements and alloys like Au ± Cu-Ag, native elements e.g. Cu, Pb and oxides (Tables 4 and 5; Fig. 8). The above minerals occur in the form of very small grains (few μm) located inside the pores of the travertines (Fig. 8).

5.2.2. Whole rock geochemical analysis

Whole rock geochemical analyses in travertine samples from all areas are presented in Table 6. The travertines from Aedipsos contain the highest concentration of a number of major and trace elements such as Na (up to 3.3 wt%), S (up to 6.78 wt%), Si (up to 950 mg/kg), Ba (up to 140 mg/kg), Cu (up to 14.7 mg/kg), Hf (up to 0.056 mg/kg), K (up to 1086 mg/kg), Pb (up to 10.6 mg/kg), Sb (up to 4.6 mg/kg), Sn (up to 0.8 mg/kg), Th (up to 0.14 mg/kg), Ti (up to 11.5 mg/kg) and Zr (up to 2 mg/kg). The maximum concentrations of As (up to 1.83 wt%) and Fe (up to 28.9 wt%) both at ore-grade, and to a lesser extent Zn (up to 24.3 mg/kg), Sc (up to 8.8 mg/kg) and Y (up to 259 mg/kg) were observed in the Ilia travertines. Finally, Li (up to 6.7 mg/kg) and Mg (up to 6850 mg/kg) are enriched in the Thermopylae travertines. The lithophile elements, like Be (up to 57.8 mg/kg), Cs (1.5 mg/kg), and U (up to 33.5 mg/kg) are enriched in the Ilia and Aedipsos travertines (Table 6).

Normalization of the whole rock chemical data to the average composition of the Upper Continental Crust (UCC, Rudnick and Gao, 2003; Fig. 9A), emphasized enrichment in several elements of the studied travertines: S, Sr and sometimes Sb, were enriched up to 10 times, arsenic especially in samples from Ilia, up to 10,000 times compared to the UCC abundances. The Ilia samples also contain 10 times more Fe, Be, B and Y than the UCC abundances.

The REE concentrations in the studied travertines are presented in Tables 6. The highest concentrations of REE occur in samples from Ilia (e.g. up to 11.9 mg/L Ce, 7.6 mg/L Nd, 3.8 mg/L Gd, 5.1 mg/L Dy, 2.9 mg/L Er, 1.9 mg/L Yb). Fig. 9B shows the normalized REE concentrations of the studied travertines to UCC. Travertines from the Ilia area demonstrate a clear enrichment of REE compared to all other samples (i.e. Aedipsos and Thermopylae). All samples show a higher enrichment to heavy REE compared to light REE. Also, all studied

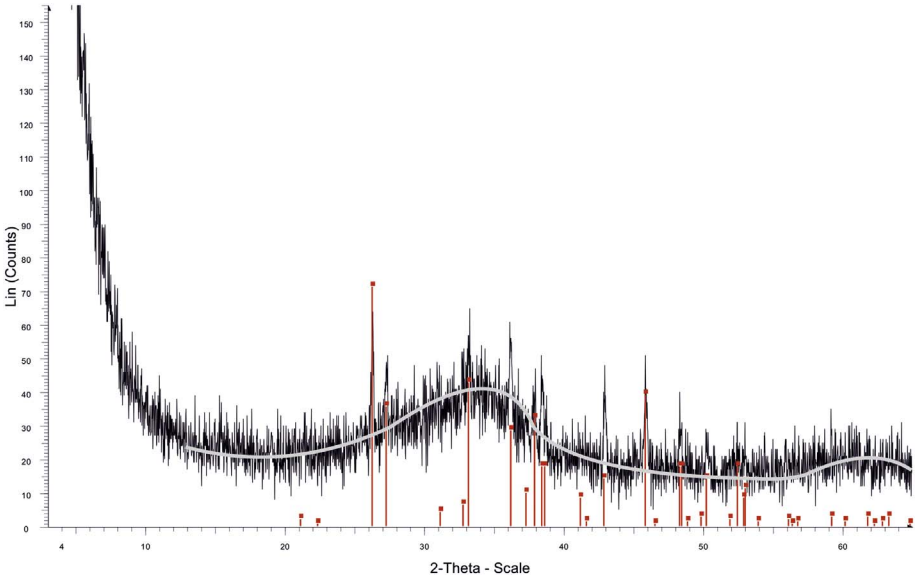

Fig. 6. XRD pattern of iron-rich material from the Ilia travertine. The background (gray thick line) shows two characteristic broad peaks at around 35° and 62° in 2θ, which are typical of poorly crystalline ferrihydrite and sharp peaks corresponding mostly to aragonite (red columns). (For interpretation of the references to color in this figure legend, the reader is referred to the web version of this article.)

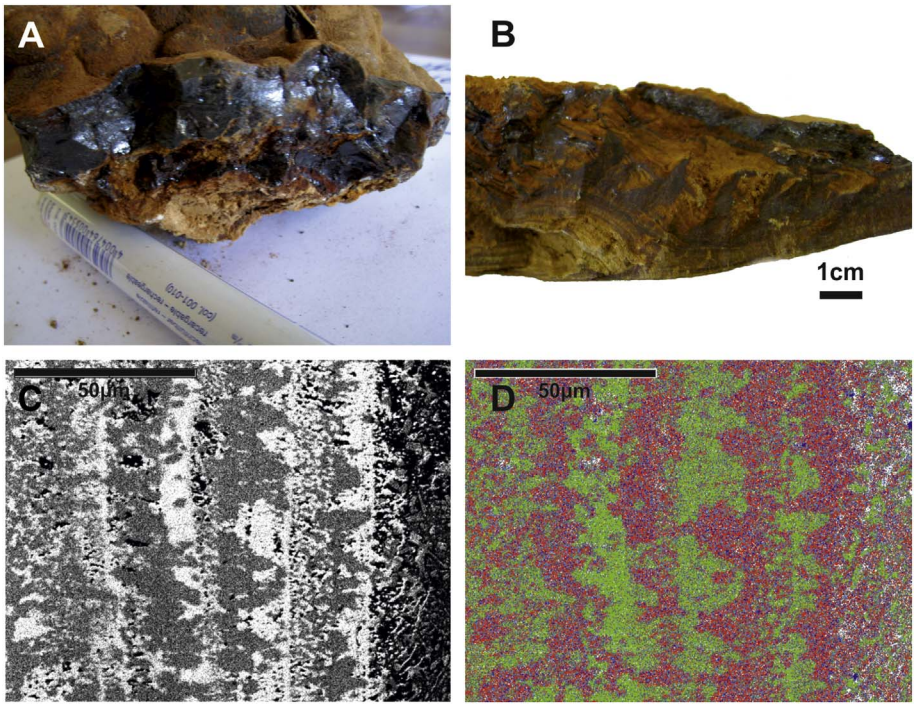

Fig. 7. Photographs demonstrating mode of occurrence of Fe ± As-rich travertines. (A and B) Hand specimens of iron rich travertine from Ilia. (C) Backscattered electron image (BSEI) of Fe-rich laminated travertine from Ilia. Black and white color showing areas with different average atomic weights. Lighter areas have a higher average atomic weight (Fe-rich) than the darker areas (Ca-rich). (D) False color BSEI, derived from the corresponding black and white BSEI, displaying the distribution of Fe (red), Ca (Green) and Si (blue). (For interpretation of the references to color in this figure legend, the reader is referred to the web version of this article.)

travertines present a slight negative anomaly in Europium (Eu). The travertines from Aedipsos and Thermopylae, also show sometimes weak negative anomaly in Cerium (Ce) and Dysprosium (Dy).

6. Discussion

6.1. Fluid characteristics of the northwestern Euboea Island and Sperchios area hydrothermal system

The hot springs in the northwestern part of Euboea island (Aedipsos, Ilia, Gialtra) and in the neighboring part of the mainland in eastern Central Greece (Sperchios area: Kamena Vourla and Thermopylae) are the surface manifestation of medium-, or possible high-enthalpy geothermal activity fed by a deep-seated magmatic chamber, which is related with the Plio-Pleistocene volcanic center of Lichades in combination with the active tectonics of the area (Chatzis et al., 2008; Karastathis et al., 2011; D'Alessandro et al., 2014; Vakalopoulos et al., 2016; Kanellopoulos et al., 2016b). A temperature of up to about 160 °C for the geothermal reservoir at Aedipsos area, was estimated on the basis of various geochemical and isotopic geothermometers by D'Alessandro et al. (2014), Dotsika (2015), Vakalopoulos et al. (2016) and Kanellopoulos et al. (2016b).

Table 4
Representative microanalyses of Au-Cu-Ag alloy (1), pyrite (2, 3), As-rich pyrite (4), arsenopyrite (5, 6), chalcopyrite (7), galena (8), sphalerite (9–11), stibnite (12 – 13).

Analysis	1	2	3	4	5	6	7	8	9	10	11	12	13
Area	IL	THE	IL	IL	THE	IL	IL	THE	IL	IL	IL	AD	AD
Ag	20.71	bdl	bdl	bdl	bdl	bdl	bdl	bdl	bdl	bdl	bdl	bdl	bdl
Pb	bdl	bdl	bdl	bdl	bdl	bdl	bdl	87.32	bdl	bdl	bdl	bdl	bdl
Fe	5.41	47.01	46.38	46.64	33.17	34.09	30.38	bdl	6.29	16.65	18.73	bdl	2.78
Cu	16.9	bdl	bdl	bdl	bdl	bdl	32.05	bdl	bdl	bdl	bdl	bdl	bdl
Zn	1.73	bdl	bdl	bdl	bdl	bdl	bdl	bdl	61.74	48.49	47.93	bdl	bdl
Au	57.19	bdl	bdl	bdl	bdl	bdl	bdl	bdl	bdl	bdl	bdl	bdl	bdl
Sb	bdl	bdl	bdl	bdl	bdl	bdl	bdl	bdl	bdl	bdl	bdl	69.37	65.22
As	bdl	bdl	bdl	1.41	44.71	44.27	bdl	bdl	bdl	bdl	bdl	bdl	bdl
Mn	bdl	bdl	bdl	bdl	bdl	bdl	bdl	bdl	bdl	1.02	0.51	bdl	bdl
S	bdl	53.46	55.32	52.65	21.49	20.75	35.3	11.84	32.5	34.8	31.23	29.5	31.97
Total	101.94	100.47	101.7	100.7	99.37	99.11	97.73	99.16	100.53	100.96	98.4	98.87	99.97
Atoms	1	3	3	3	3	3	4	2	2	2	2	5	5
Ag	0.220	0.000	0.000	0.000	0.000	0.000	0.000	0.000	0.000	0.000	0.000	0.000	0.000
Pb	0.000	0.000	0.000	0.000	0.000	0.000	0.000	1.066	0.000	0.000	0.000	0.000	0.000
Fe	0.111	1.006	0.975	1.004	0.957	0.991	1.012	0.000	0.109	0.278	0.327	0.000	0.157
Cu	0.305	0.000	0.000	0.000	0.000	0.000	0.939	0.000	0.000	0.000	0.000	0.000	0.000
Zn	0.030	0.000	0.000	0.000	0.000	0.000	0.000	0.000	0.912	0.692	0.715	0.000	0.000
Au	0.333	0.000	0.000	0.000	0.000	0.000	0.000	0.000	0.000	0.000	0.000	0.000	0.000
Sb	0.000	0.000	0.000	0.000	0.000	0.000	0.000	0.000	0.000	0.000	0.000	1.912	1.692
As	0.000	0.000	0.000	0.023	0.962	0.959	0.000	0.000	0.000	0.000	0.000	0.000	0.000
Mn	0.000	0.000	0.000	0.000	0.000	0.000	0.000	0.000	0.000	0.017	0.009	0.000	0.000
S	0.000	1.994	2.025	1.974	1.081	1.050	2.049	0.934	0.979	1.013	0.949	3.088	3.150

AD = Aedipsos, IL = Ilia, THE = Thermopylae, bdl = below detection limit.

Table 5
Metallic and non-metallic mineral phases identified in the studied travertines.

Metallic and non-metallic mineral phases	Aedipsos	Ilia	Thermopylae
Calcite	*	*	*
Aragonite	*	*	
Ferrihydrite	*	*	
Halite	*		
Sylvite	*		
Gypsum	*		
Barite	*	*	
Fluorite	*	*	
Zircon	*	*	*
Pyrite	*	*	*
Arsenopyrite	*	*	*
Galena		*	*
Sphalerite			
Fe-poor		*	*
Fe-rich		*	
Chalcopyrite		*	
Stibnite	*	*	*
Anglesite		*	*
Awaruite		*	
Native Ni			*
Native Pb		*	
Native Cu		*	
Cu-Zn(± Fe ± Sn) alloys	*	*	*
Ni-Co-Cu-Sn alloy		*	
Ni sulfide			*
Au-Ag alloys		*	
Au-Cu-Ag alloys		*	
REE minerals		*	
Cassiterite		*	
Fe-Ti oxides	*		
Fe oxides	*	*	*
Cr oxides	*		*

Previous geochemical and stable isotopic studies (Mitropoulos and Kita, 1997; Duriez et al., 2008; Chatzis et al., 2008; D'Alessandro et al., 2014; Dotsika, 2015; Kanellopoulos et al., 2016b) at the hot springs of Sperchios and Aedipsos, suggest high seawater contributions i.e. Thermopylae 22–28%, Kamena Vourla 20–43% and Aedipsos 90–94%.

Based on chemical and isotopic data (i.e. D and $\delta^{18}O$), D'Alessandro et al. (2014) and Dotsika (2015) suggested that the hot springs of Thermopylae–Kamena Vourla and Aedipsos are fed by a deep "parent" hydrothermal fluid mixed with local groundwater and seawater respectively. The deep hydrothermal fluid (for all areas) is a mixture of local groundwater (~26.3%), seawater (~56%) and magmatic water (~17.7%). For the Aedipsos area the magmatic contribution is between 5 and 10%, while in the case of Thermopylae and Kamena Vourla it is between 1.5 and 3.8% (Dotsika, 2015). This is in agreement with He isotopic analyses conducted in the area by Shimizu et al. (2005) and D'Alessandro et al. (2014). Based on isotopic composition of gas samples from Aedipsos and Thermopylae hot springs, Shimizu et al. (2005) reported $^3He/^4He$ ratios of 0.46–1.01 and 0.19 respectively and suggested that the contribution of mantle helium in Aedipsos and Thermopylae is approximately 12.5% and 3% respectively. A mixing of seawater and arc-type magmatic water was also indicated based on isotopic studies in hydrothermal fluids from hot springs from the south Aegean active volcanic arc e.g. Nisyros (Chiodini et al., 1993; Dotsika and Michelot, 1993; Brombach et al., 2003; Marini and Fiebig, 2005; Tassi et al., 2013a), Milos, Santorini, Sousaki (Dotsika et al., 2009; Tassi et al., 2013b) and Methana areas (Dotsika et al., 2010).

This study verifies previous results and classifies the hot spring samples as mature- near neutral chloride waters (Fig. 5A, B). These samples plot in the same well-defined area of a Piper diagram (Fig. 4), as water samples from other hot springs in Greece, for example those from the south Aegean active volcanic arc (Fytikas and Andritsos, 2004). Cl^- is the dominant anion in all hot water samples, with the highest concentrations observed in samples from Aedipsos (up to 2.3 wt %; seawater has 3.6 wt% Cl^-). High concentrations of conservative constituents suggest high seawater participation rates (Arnórsson, 2000). In all studied hot springs, high concentrations of conservative constituents such as B, Sr and Li were identified.

Our study on the geochemistry of the hydrothermal fluids revealed that the highest values of parameters such as pH, temperature and E.C. are always recorded in the Aedipsos and Ilia areas. Similar trends were observed in most of the analyzed anions, major and trace elements, in both the hydrothermal fluids and the travertines. The data suggest a possible spatial proximity of the Aedipsos and Ilia areas to the heat source of the hydrothermal system.

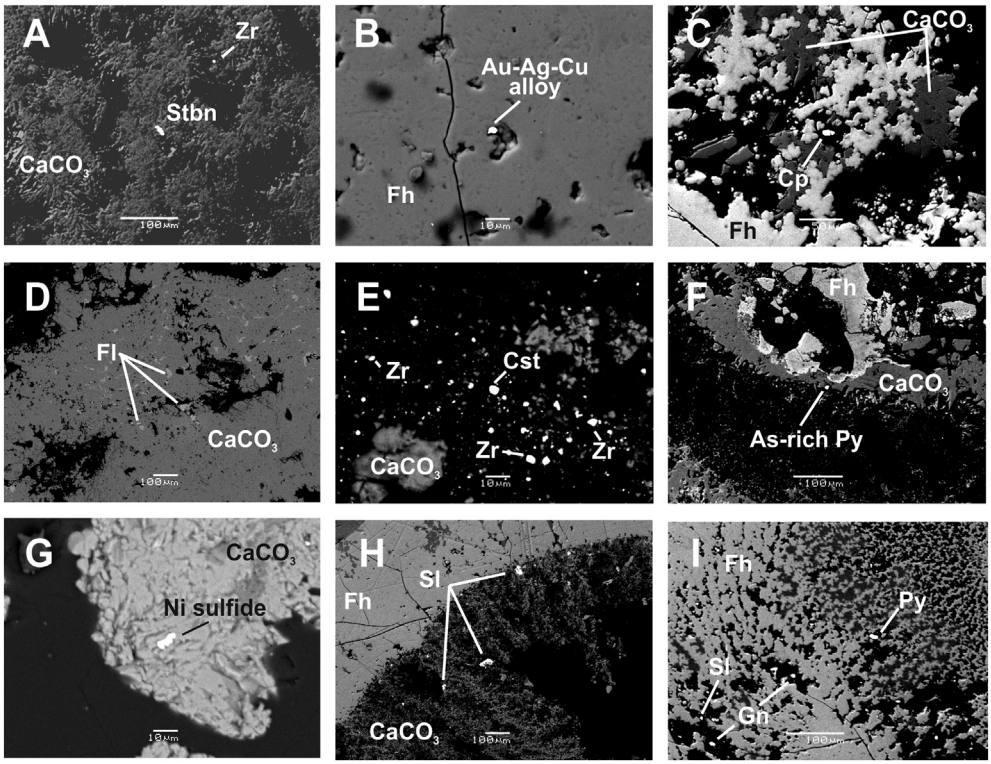

Fig. 8. Photomicrographs demonstrating ore and gangue mineralogy in the studied travertines (Backscattered electron images - BSEI). (A) Stibnite (Stbn) and zircon (Zr) inside the pores of $CaCO_3$, from Aedipsos. (B) Au-Cu-Ag alloy inside the pores of ferrihydrite (Fh) in iron rich travertine from Ilia. (C) Chalcopyrite (Cp) inside the pores of iron rich travertine from Ilia. (D) Fluorite at Aedipsos sample. (E) Cassiterite and zircon inside the pores of the $CaCO_3$ rich domain of an iron rich travertine from Ilia. (F) As-rich pyrite (Py) inside the pores of the $CaCO_3$ rich domain of an iron rich travertine from Ilia. Ferrihydrite (Fh) is also present. (G) Ni sulfide inside the pores of $CaCO_3$ from Thermopylae. (H) Sphalerite (Sl) inside the pores of $CaCO_3$ part of iron rich travertine from Ilia. (I) Sphalerite (Sl), galena (Gn) and pyrite (Py) inside the pores of ferrihydrite (Fh) in iron rich travertine from Ilia.

The chemical composition of the hydrothermal fluids has been affected by the local bedrock in several cases. The hydrothermal fluid samples from Sperchios area and especially from Kamena Vourla, show higher concentration in Co, Ni and U compared to those from Euboea. The concentrations of Co and Ni co-vary, suggesting common source (Table 2). Already, Kanellopoulos (2006, 2011) and Kanellopoulos et al. (2014a) identified similar geochemical anomalies at the cold groundwater, soils and plants and attributed this enrichment to the presence of vast occurrences of ultramafic rocks of the ophiolitic sequence and U-bearing bedrocks respectively. Also, the vast deposition of thermogenic travertines and the high Ca concentrations at Aedipsos hydrothermal fluid samples and along with drilling data (Gkioni-Stavropoulou, 1998; Chatzis et al., 2008) suggests enrichments derived from the dissolution of underlying marble/limestone sequences in the area.

However, the limited distribution of the studied samples on the characterization diagrams and also the co-variation and the limited range of their concentrations in several ions and metals, such as Na^+, K^+, Ca^{2+}, SO_4^{2-}, Cl^-, Zn and Pb reflect their chemical affinities, suggesting a common source and the fact that they belong to one single system. Based on that, and the geological setting of the area, it is possible that there is a continuation of the hydrothermal manifestations of the system in the seafloor of North Euboean Gulf, which lies between the two on-land locations.

This study demonstrates that the hydrothermal fluids mainly in the Euboea samples contain a suite of elements such as Ag, As, Ba, Cu, Cl, S, Se, Sr, Zn which are in the same order of magnitude with hydrothermal fluids from several active mineralizing hydrothermal systems elsewhere, as for example: Ngawha Well 1-New Zealand, Ahuachapan Well 20-El Salvador, Reykjanes Well H8-Iceland, Matsao Well E-205-Taiwan (Henley et al., 1986), Imperial, USA (McKibben and Hardie, 1997), Dixie, USA (Bruton et al., 1997), Cerro Pietro, Mexico (Mercado and Hurtado, 1992); Hvergerdi-Iceland, Ohtake-Japan (Ellis and Mahon, 1977), Slak, Indonesia (Gallup, 1998).

When compared with hydrothermal fluids from active hydrothermal systems depositing travertine, e.g. in the North Caucasus (Lavrushin et al., 2006) and Savo volcano, Solomon Islands (Smith, 2008), the studied fluids contain the same order of magnitude in elements like Ba, Fe, Mn, Pb, but higher concentrations in elements like As, Ca, Co, Cl, Cs, K, Mg, Na, Ni, S reflecting both the nature of fluid sources and fluid path (according to Giggenbach, 1988).

6.2. *Metallogenetic implications of the northwestern Euboea Island and Sperchios area hydrothermal system - comparison with mineralized thermogenic travertines elsewhere*

According to Sillitoe (2015), travertines may be parts of low-, and intermediate sulfidation epithermal systems, but typically are poor indicators of precious metal mineralization, due to their usually distal position relative to hydrothermal upflow zones. However, manganese and iron oxides associated with travertine may scavenge a variety of metals, generally at subeconomic levels.

In southern Tuscany (Italy), a number of carbonate-hosted “Carlin-type” gold mineralization occurs at the edges of the travertine related geothermal fields of Larderello, Amiata and Latera, areas previously known for Sb mineralization (Lattanzi, 1999). Mineralization is typically localized at the contact between carbonate rocks and overlying flysch and consists of silica replacement bodies (jasperoids) containing pyrite and stibnite. Thermogenic travertines in this area are located above Carlin-type mineralization and probably related to upflow zones of hydrothermal fluids (Lattanzi, 1999).

Travertines at the Senator mine in western Turkey contain high arsenic, derived from carbonate-hosted Sb mineralization, having affinities to Carlin-type deposits (Bernasconi et al., 1980; Nordstrom and Sharifi, 2014).

Table 6
Whole rock travertine chemistry range as determined by ICP-MS and ICP-AES analysis and comparison with travertines elsewhere.

	East. Cen. Gr.	Euboea		Russia[a]	Solomon Islands[b]	Papua New Guinea[c]
	Thermopylae (N = 2)	Aedipsos (N = 23)	Ilia (N = 3)	N. Caucasus	Savo Volcano	Tutum Bay
Ca (%)	34.2–35.3	3.2–62	10.3–21.9	0.4–49.3	32–37	37.2–38.5
Na (mg/kg)	1390–2400	700–33,100	3280–4960	bdl - 6870	140–630	370–590
P (mg/kg)	48	25–440	71–280	bdl - 756	90–410	44–87
S (mg/kg)	4670–4940	230–67,800	650–2740	30–6650	1500–10,500	bdl
Si (mg/kg)	190–200	12–950	86–340	27–8140	–	–
Al (mg/kg)	52–75	6–1150	54–150	9–7475	–	530–1800
As (mg/kg)	97–118	66–230	4895–18,300	–	0.6–626	– (up to 33,200)[d]
B (mg/kg)	17–19	3–50	73–135	bdl – 625	bdl - 36	–
Ba (mg/kg)	47–51	3–145	80–90	4–10,890	23–167	bdl - 47
Be (μg/kg)	300–380	83–2540	24,500–57,800	bdl - 47,500	–	bdl
Cd (μg/kg)	9–13	1–25	15–18	–	50–360	bdl – 400
Co (μg/kg)	bdl	bdl	bdl	bdl – 48,200	100–2900	bdl
Cr (μg/kg)	bdl	bdl	bdl	bdl - 29,000	1700	bdl
Cs (μg/kg)	320–370	20–1240	1230–1540	bdl - 77,500	–	40–14,000
Cu (μg/kg)	bdl	3600–14,700	bdl	bdl - 58,500	150–780	bdl - 18,000
Fe (mg/kg)	116–170	49–23,950	131,000–289,000	114–68,300	600–22,900	490–1260 (up to 29.7 wt%)[d]
Hf (μg/kg)	bdl	12–56	14–45	bdl - 3600	–	80–1400
K (mg/kg)	124–229	36–1090	335–510	bdl - 1270	bdl - 100	–
Li (μg/kg)	6520–6700	140–3900	1530–1940	bdl - 88,600	–	–
Mg (mg/kg)	6700–6850	87–2990	545–690	bld - 41,800	900–4300	240–540
Mn (mg/kg)	5–7	1–84	74–195	5–18,000	1260–7065	77–540
Ni (μg/kg)	bdl	bdl	bdl	bdl – 48,200	1500–4000	bdl
Pb (μg/kg)	370–530	348–10,600	720–2210	bdl – 34,600	30–1250	7000–27,000
Rb (μg/kg)	340	417–690	520–790	16–12,400		430–49,000
Sb (μg/kg)	10–16	30–4580	350–1750	bdl - 400	bdl - 90	bdl
Sc (μg/kg)	bdl	130–630	2560–8870	–	100–400	bdl
Sn (μg/kg)	bdl	90–810	bdl	–	–	–
Sr (mg/kg)	1918–2160	254–3960	2515–4260	24–13,620	1150–3970	9500–11,000
Th (μg/kg)	7–11	bdl - 150	9–41	bdl - 3700	–	30–970
Ti (μg/kg)	1920	1140–11,510	2430	–	bdl - 90,000	bld - 119,900
U (μg/kg)	23–31	10–91	75–200	bdl - 6500	bdl - 200	30–1100
V (μg/kg)	bdl	140–2560	1040–2610	bdl - 28,800	–	bdl
Y (μg/kg)	200–290	80–7980	71,100–258,900	61–86,000	–	18,000–90,000
Zn (μg/kg)	4520–4650	2520–25,900	16,000–24,300	bdl – 162,000	300–21,000	bdl
Zr (μg/kg)	180–250	29–2080	290–1070	bdl - 338,000	–	700–49,000
La (μg/kg)	bdl	180–1100	14,300–57,300	bdl - 32,100	700–2700	–
Ce (μg/kg)	100–120	19–1660	27,500–119,300	60–78,200	–	–
Pr (μg/kg)	14–15	2–220	3640–16,900	7–8400	–	–
Nd (μg/kg)	52–64	6–1110	16,700–76,500	57–31,000	–	–
Sm (μg/kg)	12–15	3–390	5280–24,400	bdl - 7200	–	–
Eu (μg/kg)	3–4	1–150	1850–8300	bdl - 1700	–	–
Gd (μg/kg)	18–20	6–770	8830–38,400	22–8700	–	–
Tb (μg/kg)	2–3	bdl - 140	1750–7580	bdl - 1600	–	–
Dy (μg/kg)	15–18	1–950	12,700–51,300	bdl - 11,900	–	–
Ho (μg/kg)	4	bdl - 190	2710–10,800	bdl - 2800	–	–
Er (μg/kg)	54–130	7–1140	7570–29,700	10–9800	–	–
Tm (μg/kg)	2	bdl - 60	940–3760	bdl - 1700	–	–
Yb (μg/kg)	6–9	2–300	5230–19,800	bdl – 11,000	–	–
Lu (μg/kg)	1	bdl - 38	650–2410	bdl - 1800	–	–

bdl = below detection limit.
[a] Lavrushin et al. (2006).
[b] Smith (2008).
[c] Pichler and Veizer (2004).
[d] Price and Pichler (2005).

In the Takab geothermal field (northwestern Iran), a considerable As enrichment in travertine and groundwaters, located in proximity to Au-As Carlin-type mineral deposits (e.g. Agdarreh deposit) has reported (Daliran, 2003, 2008; Nordstrom and Sharifi, 2014). These anomalous As concentrations were related to waning stages of Quaternary volcanic activity. Daliran (2003) reported on the presence of springs and travertines, which contain up to percent range Cu, Se, Sb, Pb, and As, up to several thousand mg/kg Hg and Te, and up to 1000 mg/kg Au and Ag. Within the Takab geothermal field, the active Angouran travertines display high concentrations in As, Ba, Zn, Cd and Ni, and considered to be formed contemporaneous and/or by remobilization of the carbonate replacement Angouran world-class Zn-Pb deposit (Boni et al., 2007; Daliran et al., 2013; Rossi et al., 2015).

In northeastern Greece, the Oligocene carbonate-replacement Pb-Zn-Cu-Ag deposit at Thermes, northeastern Greece (Arvanitidis et al., 1990; Kalogeropoulos et al., 1996) is spatially related to thermogenic travertine deposits. However, data about their mineralogical and geochemical composition is still lacking.

The Ilia iron-rich travertines show ore grade concentrations in Fe (up to 28.9 wt%) and As (up to 1.83 wt%), in accordance to their high concentration in Ilia hydrothermal fluid. The thermogenic travertines at North Caucasus (Lavrushin et al., 2006) and volcano Savo, Solomon

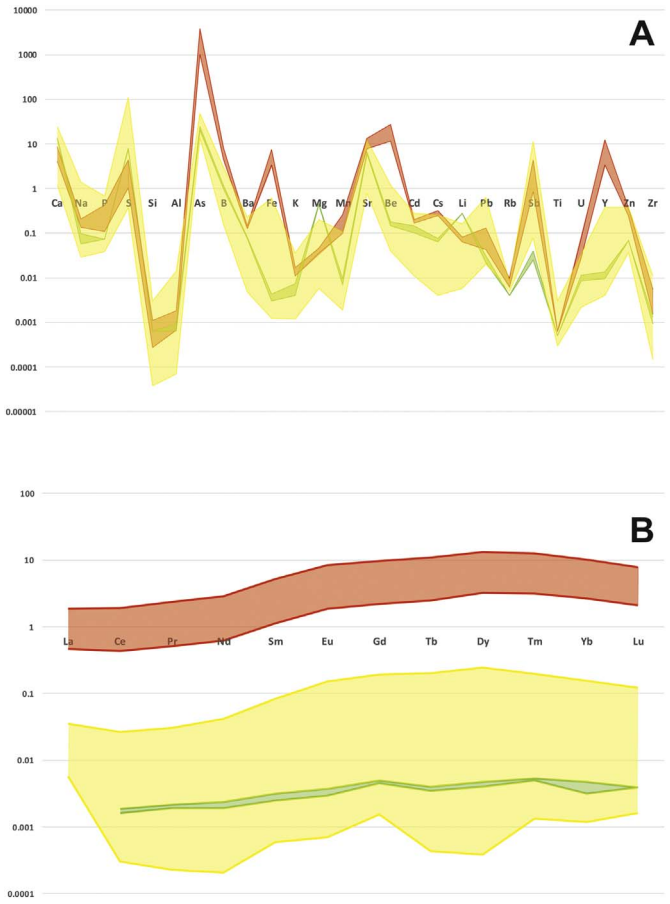

Fig. 9. ICP-MS analysis of travertine normalized against average Upper Continental Crust (Rudnick & Gao, 2003); (A) Major and trace elements. (B) REE. Yellow color represents the samples from Aedipsos, red color the samples from Ilia and green color the samples from Thermopylae. (For interpretation of the references to color in this figure legend, the reader is referred to the web version of this article.)

Islands (Smith, 2008) are associated with active metal deposition and at some chemical elements are characterized by concentrations much lower than those of the Euboea travertines, but comparable to those from Thermopylae (Table 6). The As and Fe content of the Ilia travertines are among the highest in the world, with values in North Caucasus and Savo not exceeding 626 mg/kg and 6.8 wt% respectively (Table 6). However, in the shallow submarine aragonite vent field at Tutum Bay, Ambitle island, Papua New Guinea, arsenic values (up to 3.3 wt%) and iron values (up to 29.7 wt%) measured from hydrous ferric oxides e.g. goethite, lepidocrocite, hematite and ferrihydrite that precipitate around vent edifices (Pichler and Veizer, 2004; Price and Pichler, 2005) are slightly higher than the As and Fe content in the Ilia travertines (up to 1.8 wt% As and up to 28.9 wt% Fe).

The discovery for the first time of sulfides (pyrite, arsenopyrite, galena, chalcopyrite, sphalerite, stibnite), native elements, alloys like Au ± Cu-Ag, fluorite and REE-bearing phases, syngenetically enclosed within the pores of all studied travertines, as well as of high concentrations of precious and base metals at the hydrothermal fluid (e.g. up to 10 μg/L Ag, up to 103 μg/L As, up to 1.1 wt% Fe), suggest active metallogenic processes throughout the northwestern Euboea Island and Sperchios area hydrothermal system.

This is verified by deep geothermal drilling at Aedipsos area (Chatzis et al. 2008), where active hydrothermal As-pyrite ± chalcopyrite ore deposition takes place within brecciated and silicified carbonates (i.e. jasperoids) at about 300 m below sea level (Kanellopoulos, unpublished data). Fluorite and kaolinite are additional gangue minerals.

We suggest here a scenario, where deep, reduced and low-sulfidation hydrothermal fluids (e.g. Einaudi et al. 2003; Sillitoe and Hedenquist, 2003) within the stability field of pyrite, Fe-rich sphalerite and arsenopyrite, mixed during their upflow close to the surface with cool seawater and deposited ferryhydrite. According to Pichler and Veizer (1999) precipitation of ferrihydrite could take place via oxidation of Fe^{2+} in the hydrothermal fluid, through mixing with cool, alkaline, oxygenated seawater, favored by increase of Eh and pH and decrease in temperature. Similarly to iron, part of the arsenic, which remained in the solution after deposition of sulfides at depth, was deposited together with ferrihydrite on the surface.

Based on the fact that minor amounts of metallic minerals (sulfides, alloys and native elements) are mostly located inside the pores of all studied travertines, it is suggested that they were probably formed at deeper levels of the hydrothermal system and later transferred as clastic grains by the hydrothermal fluids and gasses to the surface, where they were trapped by the fast precipitating thermogenic travertines.

The high REE content in Ilia iron-rich travertine (up to ~465 mg/kg ΣREE) is caused by adsorption of REE-bearing phases by iron oxyhydroxides, similarly to that described at Tutum Bay, Papua New Guinea, where rare earth elements are known to be very effectively adsorbed by Fe^{3+} oxyhydroxides (Pichler and Veizer, 1999).

There are several mineralogical and geochemical observations supporting the hypothesis of magmatic contribution to the studied hydrothermal system: (i) the presence of elements in their native form (e.g. Pb, Cu) which according to Rychagov, 2005, Rychagov et al., 2006 are indicative for injection of a high-temperature magmatic fluid in geothermal reservoirs; (ii) the presence of native alloys (e.g. Au ± Cu-Ag), and the enrichment of metalloids (e.g. As, Sb), which according to Williams-Jones and Heinrich (2005) and Saunders et al. (2016) highlight a transport as magmatic vapors from deep magmatic sources to the epithermal environment; (iii) the abundance of REE which may suggest a magmatic-related origin to hydrothermal deposits (Ciobanu et al., 2006; Voudouris et al., 2013).

We support the hypothesis that metals and metalloids in the study area were mainly derived from magmatic fluids, which after mixing with heated sea waters deposited sulfide mineralization at depth, and As-enriched hydrous iron oxides in the studied travertines at the surface. In this respect, the northwestern Euboea Island and Sperchios area hydrothermal system represents the first documented active terrestrial mineralizing hydrothermal system associated with ore-bearing travertines in Greece. Until now only shallow submarine hot springs across the south Aegean active volcanic arc were reported, where inputs of metals like Fe, Mn, As and Sb into surficial sediments have been found within the Santorini caldera and at Paleochori Bay, Milos island (Valsami-Jones et al., 2005; Kilias et al., 2013).

Based on the available data a precise classification of the mineralization at depth is not possible. The metallic and gangue mineralogy present in the Aedipsos, Ilia and Thermopylae travertines and in the deep geothermal drill core at Aedipsos (As-rich pyrite, minor chalcopyrite, fluorite and presence of jasperoids) indicate remobilization from carbonate-hosted sulfide mineralization, similarly to that described above for Tuscany and northwestern Iran and suggest that the study area has potential for future base and precious metal discoveries.

7. Conclusions

The northern Euboea island and neighboring parts of the mainland in eastern Central Greece, i.e. the Sperchios area, contain several hot springs and thermogenic travertine deposits, which are surface manifestations of a single active hydrothermal system, most likely extending offshore within the Northern Euboean Gulf in a unique geological position at the back-arc region of the south Aegean active volcanic arc and at the western extremity of North Anatolian fault.

i. High content of precious and base metals in the hydrothermal fluids (e.g. up to 10 μg/L Ag, up to 103 μg/L As, up to 1.1 wt% Fe),

suggest active ore mineralizing processes throughout the area. The observed limited variability in elemental concentrations of the hydrothermal fluids (e.g. Co, Ni and U in Kamena Vourla or Fe and As at Ilia), are attributed mainly to localized influence of the subsurface lithology.

ii. The geochemical composition of the hydrothermal fluids is directly reflected in the metallic mineral phases identified in the travertines and the lithogeochemistry of the travertines. Typical example is the Fe ± As -rich (i.e. ferrihydrite-bearing) travertine in the Ilia area, which shows ore grade concentrations in Fe (up to 28.9 wt%) and As (up to 1.83 wt%), reflecting their high concentrations in the Ilia hydrothermal fluid.

iii. Minor amounts of metal-bearing minerals such as pyrite, arsenopyrite, galena, chalcopyrite, sphalerite, stibnite, elements in their native form such as Pb, Ni, alloys such as Au ± Cu-Ag, fluorite and REE-bearing phases, discovered for the first time, are syngenetically enclosed as clastic grains within the pores of all studied travertines, and were probably formed at deeper levels of the hydrothermal system, as carbonate-hosted sulfide mineralization, and later remobilized and transferred by the hydrothermal fluids to the surface. The high REE content in Ilia Fe ± As-rich travertines (up to ~465 mg/kg ΣREE) is caused by incorporation of REE-bearing phases by the iron oxyhydroxides.

iv. For the formation of Fe ± As-rich travertines we suggest a scenario, where reduced and low-sulfidation state hydrothermal fluids within the stability field of pyrite, Fe-rich sphalerite and arsenopyrite at depth, mixed close to the surface with cool seawater and deposited ferrihydrite. A magmatic contribution is suggested by the presence of elements in their native form such as Pb, Cu, alloys such as Au ± Cu-Ag, metalloids such as As, Sb, and REE-bearing minerals in thermogenic travertines.

v. The northwestern Euboea Island and Sperchios area hydrothermal system represents the first documented active terrestrial mineralizing hydrothermal system associated with ore-bearing travertines in Greece.

Acknowledgements

The corresponding author would like to thank the local authorities, the local population and especially the Director of the Public Properties Company - Aedipsos branch, Mr. Ilia Siakantari, for their co-operation during the field work. Also, the Dr. Deborah Berhanu, Dr. Superb Misra, Dr. Stanislav Strekopytov and Catherine Unsworth of the Natural History Museum are acknowledged for their support during the chemical and mineralogical analyses. And finally, the two anonymous reviewers and Associate Editor Alecos Demetriades are acknowledged for their thorough review and useful comments and suggestions that greatly improved the quality of the paper.

References

Angelopoulos, I., Mitropoulos, D., Perissoratis, C., Zimianitis, E., 1991. Pagasitikos sheet, 1:200,000. In: Surficial Sediment Map of the Aegean Sea Floor. I.G.M.E., Athens.

Arnórsson, S., 2000. Isotopic and chemical techniques in geothermal exploration, development and use. In: Sampling Methods, Data Handling, Interpretation. International Atomic Energy Agency, Vienna 351 pp.

Arvanitidis, N., Constantinides, D., Perdikatsis, V., Favas, N., Romaidis, I., 1990. Gold Ore-prospecting of the Thrust Plane Controlled Jasperoidal Rocks in the Thermes Ore-field. IGME, Xanthi Branch, pp. 36 in Greek with English abstract.

Athanasoulis, K., Vakalopoulos, K., Xenakis, M., Persianis, D., Taktikos, S., 2009. Periodical Monitoring of Hot Springs of Greece. I.G.M.E., Athens (In Greek).

Athanasoulis, K., Vougioukalakis, G., Xenakis, M., Kavouri, K., Kanellopoulos, C., Christopoulou, M., Statha, F., Rigopoulos, P., Spagakos, N., Tsigkas, Th., Papadatou, M., 2016. Diachronic Monitoring of Hot Springs and Geothermal Fields of Greece. I.G.M.E., Athens (In Greek).

Aubouin, J., 1959. Contribution a l'étude géologique 'de la Gréce septentrionale: Les confins de l'Epire et de la Thessalie. Ann. Géol. Pays Hellen 10, 1–483.

Barnes, H.L., 1997. Geochemistry of Hydrothermal Ore Deposits, third ed. Wiley - Inter Science, Inc., New York.

Barnes, H.L., 2015. Hydrothermal processes. Geochem. Perspect. 4 (1), 1–93.

Bellon, H., Jarrige, J.J., Sorel, D., 1979. Les activites magmatiques egeennes de l'oligocene a nos jours et leurs cadres geodynamiques. Donnees nouvelles et synthese. Rev. Géol. Dynam. Géog. Phys. 21, 41–55.

Bernasconi, A., Glover, N., Viljoen, R.P., 1980. The geology and geochemistry of the senator antimony deposit - Turkey. Miner. Deposita 15, 259–274.

Boni, M., Gilg, H.A., Balassone, G., Schneider, J., Allen, C.R., Moore, F., 2007. Hypogene Zn carbonate ores in the Angouran deposit, NW Iran. Miner. Deposita 42. pp. 799–820.

Brombach, T., Caliro, S., Chiodini, G., Fiebig, J., Hunziker, J., Raco, B., 2003. Geochemical evidence for mixing of magmatic fluids with seawater, Nisyros hydrothermal system, Greece. Bull. Volcanol. 65, 505–516.

Brown, K.L., 1986. Gold Deposition from Geothermal Discharges in New Zealand: Economic Geology. 81. pp. 979–983.

Bruton, C.J., Moore, J.N., Powell, T.S., 1997. Geochemical analysis of fluid-mineral relations in the Tiwi geothermal field, Philippines. In: Proceedings of the 22nd Stanford Workshop on Geothermal Reservoir Engineering, pp. 457–463.

Celet, P., 1962. Contribution a l'étude géologique du Parnasse-Kiona et d'une partie des regions méridionales de la Gréce continentale. Ann. Géol. Pays Hellén XIII, 1–446.

Chatzis, M., Kavouridis, Th., Vakalopoulos, P., Xenakis, M., 2008. Research and Identification of Geothermal Fields in Northern Euboea. I.G.M.E, Athens (in Greek).

Chiodini, G., Cioni, R., Leonis, C., Marini, L., Raco, B., 1993. Fluid geochemistry of Nisyros island, Dodecanese, Greece. J. Volcanol. Geotherm. Res. 56, 95–112.

Ciobanu, C.L., Cook, N.L., Damian, F., Damian, G., 2006. Gold scavenged by bismuth melts: an example from Alpine shear-remobilizates in the Highis Massif, Romania. Mineral. Petrol. 87, 351–384.

Clarke, P.J., Davies, R.R., England, P.C., Parsons, B., Billiris, H., Paradissis, D., Veis, G., Cross, P.A., Denys, P.H., Ashkenazi, V., Bingley, R., Kahle, H.G., Muller, M.V., Briole, P., 1998. Crustal strain in central Greece from repeated GPS measurements in the interval 1989-1997. Geophys. J. Int. 135, 195–214.

Clesceri, L., Greenberg, A., Eaton, A., 1989. Standard Methods for the Examination of Water and Wastewater, 20th ed. APHA-AWWA-WEF, Washington, DC.

D'Alessandro, W., Brusca, L., Kyriakopoulos, K., Bellomo, S., Calabrese, S., 2014. A geochemical traverse along the "Sperchios Basin e Evoikos Gulf" graben (Central Greece): Origin and evolution of the emitted fluids. Mar. Pet. Geol. 55, 295–308.

Daliran, F., 2003. Discovery of 1.2 kg/t gold and 1.9 kg/t silver in mud precipitates of a cold spring from the Takab geothermal field, NW Iran. In: Eliopoulos, D. (Ed.), Mineral Exploration and Sustainable Development. Millpress, Rotterdam, pp. 65–68.

Daliran, F., 2008. The carbonate rock-hosted epithermal gold deposit of Agdarreh, Takab geothermal field, NW Iran - hydrothermal alteration and mineralization. Miner. Deposita 43, 383–404.

Daliran, F., Pride, K., Walther, J., Berner, Z.A., Bakker, R.J., 2013. The Angouran Zn (Pb) deposit, NW Iran. Ore Geol. Rev. 53, 373–402.

Dando, P.R., Stiiben, D., Varnavas, S.P., 1999. Hydrothermalism in the Mediterranean Sea. Prog. Oceanogr. 44, 333–367.

Dotsika, E., 2015. H-O-C-S isotope and geochemical assessment of the geothermal area of Central Greece. J. Geochem. Explor. http://dx.doi.org/10.1016/j.gexplo.2014.11.008.

Dotsika, E., Michelot, J.L., 1993. Hydrochemistry, isotopic ratios and origin of geothermal fluids of Nisyros. Bull. Soc. Geol. Gr. XXVII (2), 293–304 (in Greek).

Dotsika, E., Poutoukis, D., Michelot, J.L., Raco, B., 2009. Natural tracers for identifying the origin of the thermal fluids emerging along the Aegean Volcanic Arc (Greece): evidence of arc-type magmatic water (ATMW) participation. J. Volcanol. Geotherm. Res. 179, 19–32.

Dotsika, E., Poutoukis, D., Raco, B., 2010. Fluid geochemistry of the Methana Peninsula and Loutraki geothermal area, Greece. J. Geochem. Explor. 104, 97–104.

Duriez, A., Marlin, C., Dotsika, E., Massault, M., Noret, A., Morel, J.L., 2008. Geochemical evidence of seawater intrusion into a coastal geothermal field of central Greece: example of the Thermopylae system. Environ. Geol. 54 (3), 551–564.

Einaudi, M.T., Hedenquist, J.W., Inan, E.E., 2003. Sulfidation state of fluids in active and extinct hydrothermal systems: transitions from porphyry to epithermal environments. 10. Society of Economic Geologistspp. 285–313 Special Publication.

Ellis, A.J., Mahon, W.A.J., 1977. Chemistry and Geothermal Systems. Academic Press, New York 392 p.

Fytikas, M., Andritsos, N., 2004. Geothermia. Tziola Publ., Athens (in Greek).

Fytikas, M., Kolios, N., 1979. Preliminary heat flow map of Greece. In: Cermak, V., Rybach, L. (Eds.), Terrestrial Heat Flow in Europe. Springer-Verlag, pp. 197–205.

Fytikas, M., Giuliani, O., Innocenti, F., Marinelli, G., Mazzuoli, R., 1976. Geochronological data on recent magmatism of the Aegean Sea. Tectonophysics 31, T29–T34.

Gallup, D.L., 1998. Geochemistry of geothermal fluids and well scales and potential for mineral recovery. Ore Geol. Rev. 12, 225–236.

Gartzos, E., Stamatis, G., 1996. Genesis of the thermal springs of Sperchios graben, Greece. In: Neues Jahrbuch für Geologie und Paläontologie, Mh, pp. 91–115 1996/H2.

Georgalas, G.C., 1938. Les volcans des îles Likhades et de Hagios Ioannis (Kammena Vourla). Praktika Academia Athinion 13, 86–98.

Georgiades, A.N., 1958. Sur une nouveau centre volcanique pleistocène sur la route de Volo à Almyros en Théssalie. Praktika Academia Athinion 33, 257–269.

Giggenbach, W.F., 1997. The origin and evolution of fluids in magmatic-hydrothermal systems. In: Barnes, H.L. (Ed.), Geochemistry of Hydrothermal Ore Deposits, 3rd edition. John Wiley and Sons, pp. 737–796.

Giggenbach, W.F., 1988. Geothermal solute equilibria. Derivation of Na–K–Ca–Mg geoindicators. Geochim. Cosmochim. Acta 52, 2749–2765.

Gkioni-Stavropoulou, G., 1983. Inventory of hot and mineral springs of Greece, I, Aegean Sea. In: Hydrological and Hydrogeological Investigation Report No. 39. IGME, Athens (in Greek).

Gkioni-Stavropoulou, G., 1998. Hydrogeological Study of hot and Mineral Springs of Euboean – Maliac Gulf. IGME, Athens (in Greek).
Goldberg, E.D., 1963. The oceans as a chemical system. In: Hill, M.N. (Ed.), The composition of seawater. Comparative and descriptive oceanography. The sea: ideas and observations on progress in the study of the seas 2. pp. 3–25.
Hannington, M.D., Scott, S.D., 1988. Mineralogy and geochemistry of a hydrothermal silica-sulfide-sulfate spire in the caldera of Axial Seamount, Juan de Fuca Ridge. Can. Mineral. 26, 603–625.
Henley, R.W., 1985. The geothermal framework for epithermal deposits. Rev. Econ. Geol. 2, 1–24.
Henley, R.W., Ellis, A.J., 1983. Geothermal systems, ancient and modem: a geochemical review. Earth Sci. Rev. 19, 1–50.
Henley, J.J., Cygan, G.L., d'Angelo, W.M., 1986. Effect of pressure on ore mineral solubilities under hydrothermal conditions. Geology 14, 377–379.
Imai, H., Adachi, M., Takahashi, M., Yamaguchi, M., Yashiro, K., 1988. Sulfide mineralization in the Oku-Aizu geothermal field, with the genetical relation to the epithermal gold deposits. J. Min. Geol. 38, 291–301.
Innocenti, F., Agostini, S., Doglioni, C., Manetti, P., Tonarini, S., 2010. Geodynamic evolution of the Aegean: constraints from the Plio-Pleistocene volcanism of the Volos–Evia area. J. Geol. Soc., London 167, 475–489.
Jolivet, L., Faccenna, C., Huet, B., Labrousse, L., Le Pourhiet, L., Lacombe, O., Lecomte, E., Burov, E., Denèle, Y., Brun, J.-P., Philippon, M., et al., 2013. Aegean tectonics: Strain localisation, slab tearing and trench retreat. Tectonophysics 597-598, 1–33.
Kalogeropoulos, S.I., Kilias, S., Arvanitidis, N., 1996. Physicochemical conditions of deposition and origin of carbonate-hosted base metal sulphide mineralization Thermes ore-field, Rhodope Massif, NE Greece. Miner. Deposita 31, 407–418.
Kanellopoulos, C., 2006. Geochemical Research on the Distribution of Metallic and Other Elements to the Groundwater in Fthiotida Prefecture and N. Euboea. Master Thesis National and Kapodistrian University of Athens, Greece (in Greek).
Kanellopoulos, C., 2011. Geochemical research on the distribution of metallic and other elements in the cold and thermal groundwater, soils and plants in Fthiotida Prefecture and N. Euboea. Environmental impact National and Kapodistrian University of Athens, Greece Ph.D. Thesis. in Greek with English abstract.
Kanellopoulos, C., 2012. Distribution, lithotypes and mineralogical study of newly formed thermogenic travertines in northern Euboea and eastern central Greece. Central European Geosciences 4 (4), 545–560.
Kanellopoulos, C., 2013. Various morphological types of thermogenic travertines in northern Euboea and eastern central Greece. Bull. Geol. Soc. Greece XLVII (3), 1929–1938.
Kanellopoulos, C., 2014b. Morphological types, lithotypes, mineralogy and possible bio-mineralization processes in simple and iron-rich travertines from active thermogenic travertine-forming systems in Greece. The cases of Northern Euboea and Eastern Central Greece. In: 19th International Sedimentological Congress-Abstracts Book, pp. 341.
Kanellopoulos, C., Mitropoulos, P., Argyraki, A., 2014a. Geochemical effect of ultrabasic ophiolitic rock chemistry and anthropogenic activities on groundwater contamination: the case of Atalanti area, Greece. Bul. Shk. Gjeol. 2, 329–332 Special Issue.
Kanellopoulos, C., Christopoulou, M., Xenakis, M., Vakalopoulos, P., 2016b. Hydrochemical Characteristics and Geothermometry Applications of hot Groundwater in Aedipsos Area, NW Euboea (Evia), Greece. Bull. Geol. Soc. 720–729 (Greece, L).
Kanellopoulos, C., Lamprinou, V., Mitropoulos, P., Voudouris, P., 2016a. Thermogenic travertine deposits in Thermopylae hot springs (Greece) in association with cyanobacterial microflora. Carbonates and Evaporates Journal 31 (3), 239–248.
Karabelas, A.J., Andritsos, N., Mouza, A., Mitrakas, M., Vrouzi, F., Christanis, K., 1989. Characteristics of scales from the Milos geothermal plant. Geothermics 18, 169–174.
Karagiannis, P., Pentarakis, L., Pippos, X., Futikas, M., 1990. Study for the Evaluation, Development and Utilization of Geothermal Fields in the Country. Y.B.E.. (in Greek).
Karastathis, V.K., Papoulia, J., Di Fiore, B., Makris, J., Tsambas, A., Stampolidis, A., Papadopoulos, G.A., 2011. Deep structure investigations of the geothermal field of the North Euboean Gulf, Greece, using 3-D local earthquake tomography and Curie Point depth analysis. J. Volcanol. Geotherm. Res. 206, 106–120.
Katsikatsos, G., Mettos, A., Vidakis, M., 1984. Geological map of Istiea, scale 1: 50,000. Institute of Geological and Mineral Exploration (I.G.M.E.), Athens.
Kilias, S.P., Nomikou, P., Papanikolaou, D., Polymenakou, P.N., Godelitsas, A., Argyraki, A., Carey, S., Gamaletsos, P., Mertzimekis, T.J., Stathopoulou, E., Goettlicher, J., Steininger, R., Betzelou, K., Livanos, I., Christakis, C., Bell, K.C., Scoullos, M., 2013. New insights into hydrothermal vent processes in the unique shallow-submarine arc-volcano, Kolumbo (Santorini), Greece. Nat. Sci. Rep. 3, 2421.
Kranis, H., 1999. Neotectonic activity of Fault Zones in central-eastern mainland Greece (Lokris). Ph.D. Thesis National and Kapodistrian University of Athens, Greece (in Greek).
Kranis, H., 2007. Neotectonic basin evolution in central-eastern mainland Greece. Bull. Geol. Soc. Greece 40, 360–373.
Lambrakis, N., Kallergis, G., 2005. Contribution to the study of Greek thermal springs: hydrogeological and hydrochemical characteristics and origin of thermal waters. J. Hydrogeol. 13, 506–521.
Lattanzi, P., 1999. Epithermal precious metal deposits of Italy – an overview. Miner. Deposita 34, 630–638.
Lavrushin, V., Kuleshov, V., Kikvadze, O., 2006. Travertines of the Northern Caucasus. Lithol. Miner. Resour. 41 (2), 137–164.
Lebedev, L.M., 1973. Minerals of contemporary hydrotherms at Cheleken. Geochem. Int. 9, 485–504.
Margomenou-Leonidopoulou, G., 1976. Preliminary report of the research of Aedipsos thermometallic waters. In: Proc. of the International Congress on Thermal Waters. Geothermal Energy and Volcanism of the Mediterranean area, Athenspp. 340–351.
Marini, L., Fiebig, J., 2005. Fluid geochemistry of the magmatic-hydrothermal system of Nisyros (Greece). In: Hunziker, J.C., Marini, L. (Eds.), The Geology, Geochemistry and Evolution of Nisyros Volcano (Greece). Implications for the volcanic hazards 44. Memoires de Géologie, Lausanne, pp. 121–163.
McKenzie, D., 1970. Plate tectonics of the Mediterranean region. Nature 226, 239–242.
McKenzie, D., 1972. Active tectonics of the Alpide – Himalayan belt: the Aegean Sea and surrounding regions (tectonics of the Aegean Region). Geophys. J. Roy. Astron. Soc. 55, 217–254.
McKibben, M.A., Hardie, L.A., 1997. Ore-forming brines in active continental rifts. In: Barnes, H.L. (Ed.), Geochemistry of Hydrothermal ore Deposits. John Wiley & Sons, New York, NY, United States, pp. 877–935.
McKibben, M.A., Williams, A.E., Hall, G.E.M., 1989. Precious metals in the Salton Sea geothermal brines. Geothermal Resour. Council Trans. 13, 45–47.
Mercado, S., Hurtado, R., 1992. Potash extraction from Cerro Prieto geothermal brine. Geothermics 21, 759–764.
Mercado, S., Bermejo, F., Hurtado, R., Terrazas, B., Hernándes, L., 1989. Scale incidence on production pipes of Cerro Prieto geothermal wells: Geothermics. 18. pp. 225–232.
Minissale, A., Duchi, V., Kolios, N., Totaro, G., 1989. Geochemical characteristics of Greek thermal springs. J. Volcanol. Geotherm. Res. 39, 1–16.
Mitropoulos, P., Kita, I., 1997. Geochemistry of oxygen and hydrogen isotopes in Greek regional waters. In: Proc 4th Hydrogeol. Congr., Hydrogeol. Commission of Greece, Athens, pp. 285–291.
Mountrakis, D., 1986. The Pelagonian zone in Greece: A polyphase deformed fragment of the Cimmerian continent and its role in the geotectonic evolution of the Eastern Mediterranean. J. Geol. 94, 335–347.
Nordstrom, D.K., Sharifi, R., 2014. Recent studies of arsenic mineralization in Iran and its effect on water and human health. In: One Century of the Discovery of Arsenicosis in Latin America (1914–2014). Proceedings of the 5th International Congress on Arsenic in the Environment, Buenos Aires, Argentina. CRC Press, pp. 345–348.
Orfanos, G., 1985. Inventory of hot and mineral springs of Greece, Peloponnesus, Zakynthos, Kythira. In: Hydrological and Hydrogeological Investigation Report No. 39. IGME, Athens (in Greek).
Orfanos, G., Sfetsos, K.S., 1975. Hydrogeological Study of Kamena Vourla Area. IGME, Athens (in Greek).
Palyvos, N., Bantekas, I., Kranis, H., 2006. Transverse fault zones of subtle geomorphic signature in northern Evia island (central Greece extensional province): an introduction to the Quaternary Nileas graben. In: Geomorphology. 76. pp. 363–374.
Pe-Piper, G., Piper, D., 2002. The Igneous Rocks of Greece, the Anatomy of an Orogen. Gebruder Borntraeger, Berlin.
Pertessis, M., 1961. Relations entre la composition chimique des sources thermominerales en Grece et la constitution geologique du pays. In: Groundwater in Arid Zones - Symposium of Athens. IAHS Redbooks. 57. pp. 651–656.
Pichler, T., Veizer, J., 1999. The chemical composition of shallow-water hydrothermal fluids in Tutum Bay, Ambitle Island, Papua New Guinea and their effect on ambient seawater. Mar. Chem. 64, 229–252.
Pichler, T., Veizer, J., 2004. The precipitation of aragonite from shallow-water hydrothermal fluids in a coral reef, Tutum Bay, Ambitle Island, Papua New Guinea. Chem. Geol. 207, 31–45.
Pirajno, F., 2009. Hydrothermal Processes and Mineral Systems: East Perth, Australia. Springer (1250 p).
Price, R.E., Pichler, T., 2005. Distribution, speciation and bioavailability of arsenic in a shallow-water submarine hydrothermal system, Tutum Bay, Ambitle Island. Chem. Geol. 224, 122–135.
Price, R.E., Savov, I., Planer-Friedrich, B., Bühring, S.I., Amend, J., Pichler, T., 2013. Processes influencing extreme As enrichment in shallow-sea hydrothermal fluids of Milos Island, Greece. Chem. Geol. 348, 15–26.
Ramsey, M.H., Thompson, M., Banerjee, E.K., 1987. A realistic assessment of analytical data quality from inductively coupled plasma atomic emission spectrometry. Anal. Proc. 24, 260–265.
Rossi, M., Gasquet, D., Develle, A.L., Daliran, F., Lécuyer, C., Fourel, F., Ghalamghash, J., Jafari-Saroughi, H.R., Ardebili, O., 2015. Evidence of ore remobilization by thermal waters: example from the active geothermal field of Takab and Angouran, NW Iran. In: Proceedings of the 13th SGA Meeting, Nancy (France). 2. pp. 533–536.
Rudnick, R.L., Gao, S., 2003. Composition of the continental crust. In: Rudnick, R.L. (Ed.), The Crust. 3. Elsevier, pp. 1–64.
Rychagov, S.N., 2005. Hydrothermal–magmatic systems of island arcs: the structure and stages development. In: Proceedings of International Kuril–Kamchatka Field Workshop 7 “Geothermal and Mineral Resources of Modern Volcanism Areas”, Petropavlovsk Kamchatsky, pp. 117–140 (in Russian).
Rychagov, S., Belousov, V., Sandimirova, E., Davletbayev, R., 2006. Hydrothermal ore minerals: composition, distribution and formation conditions in a conductive geothermal environment. In: International Mineral Extraction from Geothermal Brines Conference.
Sakellariou, D., Rousakis, G., Kaberi, H., Kapsimalis, V., Georgiou, P., Kanellopoulos, Th., Lykousis, V., 2007. Tectono-sedimentary structure and Late Quaternary evolution of the North Evia Gulf basin, central Greece: preliminary results. Bull. Geol. Soc. 451–462 (Greece, XL).
Saunders, J.A., Brueseke, M.E., Mathur, R., Kamenov, G.D., Shimizu, T., 2016. New isotopic evidence bearing on bonanza (Au-Ag) epithermal ore-forming processes. Miner. Deposita 51, 1–11.
Scherreiks, R., 2000. Platform margin and oceanic sedimentation in a divergent and convergent plate setting (Jurassic, Pelagonian Zone, NE Evvoia, Greece). Int. J. Earth Sci. 89, 90–107.
Sfetsos, K.S., 1988. Inventory of hot and mineral springs of Greece, III, Mainland Greece. In: Hydrological and Hydrogeological Investigation Report No. 39. IGME, Athens (in

Greek).
Shaw, B., Jackson, J., 2010. Earthquake mechanisms and active tectonics of the Hellenic subduction zone. Geophys. J. Int. 181, 966–984.
Shimizu, H., Sumino, K., Nagao, K., Notsu, K., Mitropoulos, P., 2005. Variation in noble gas isotopic composition of gas samples from the Aegean arc, Greece. J. Volcanol. Geotherm. Res. 140 (4), 321–339.
Sillitoe, R.H., 2015. Epithermal paleosurfaces. Miner. Deposita 50, 767–793.
Sillitoe, R.H., Hedenquist, J.W., 2003. Linkages between volcano tectonic settings, ore-fluid compositions, and epithermal precious metal deposits. Soc. Econ. Geol. Spec. Pub. 10, 315–343.
Smith, D., 2008. From slab to sinter: the magmatic-hydrothermal system of Savo volcano, Solomon Islands. PhD Thesis University of Leicester, U.K.
Tassi, F., Capecchiacci, L., Gianninia, G.E. Vougioukalakis, Vaselli, O., 2013a. Volatile organic compounds (VOCs) in air from Nisyros Island (Dodecanese archipelago, Greece): Natural versus anthropogenic sources. Environ. Pollut. 180, 111–121.
Tassi, F., Vaselli, O., Papazachos, C.B., Giannini, L., Chiodini, G., Vougioukalakis, G.E., Karagianni, E., Vamvakaris, D., Panagiotopoulos, D., 2013b. Geochemical and isotopic changes in the fumarolic and submerged gas discharges during the 2011–2012 unrest at Santorini caldera (Greece). Bull. Volcanol. 75, 711–726.
Tzitziras, A., Ilias, P., 1996. Geotechnical Study of Loutra Aedipsos Peripheral Road. IGME, Athens (in Greek).
Vakalopoulos, P., Metaxas, A., Xenakis, M., 2000. Research and Evaluation of Lignite Resources in Euboea Island: Northern Euboea Basin. Report of IGMEpp. 35 (in Greek).
Vakalopoulos, P., Xenakis, M., Vougioukalakis, G., Kanellopoulos, C., Christopoulou, M., Statha, F., 2016. Medium–High Enthalpy Geothermal Exploration in Aedipsos Area. I.G.M.E., Athens (In Greek).
Valsami-Jones, E., Baltatzis, E., Bailey, E.H., Boyce, A.J., Alexander, J.L., Magganas, A., Anderson, L., Waldron, S., Ragnarsdottir, K.V., 2005. The geochemistry of fluids from an active shallow submarine hydrothermal system: Milos island, Hellenic Volcanic Arc. J. Volcanol. Geotherm. Res. 148, 130–151.
Vavassis, I., 2001. Geology of the Pelagonian zone in northern Evia Island (Greece): Implications for the geodynamic evolution of the Hellenides. These de Doctorat, Univ. de Lausanne, Switzerland.
Vött, A., 2007. Relative sea level changes and regional tectonic evolution of seven coastal areas in NW Greece since the mid-Holocene. Quat. Sci. Rev. 26 (7–8), 894–919.
Voudouris, P., Spry, P.G., Mavrogonatos, C., Sakellaris, G.A., Bristol, S.K., Melfos, V., Fornadel, A., 2013. Bismuthinite derivatives, lillianite homologues, and bismuth sulfotellurides as indicators of gold mineralization at the Stanos shear-zone related deposit, Chalkidiki, northern Greece. Can. Mineral. 51, 119–142.
Weissberg, B.G., Browne, P.R.L., Seward, T.M., 1979. Ore metals in active geothermal systems. In: Barnes, H.L. (Ed.) Geochemistry of Hydrothermal Ore Deposits. Third edition, Wiley-Interscience, Inc., New York, Chapter 15, 738–780.
White, D.E., 1955. Violent mud-volcano eruption of Lake City Hot Springs, northeastern California. Geol. Soc. Am. Bull. 66, 1109–1130.
White, D.E., 1981. Active geothermal systems and hydrothermal ore deposits. In: Economic Geology 75th Anniversary Volume, pp. 392–423.
Williams-Jones, A.E., Heinrich, C.A., 2005. Vapor transport of metals and the formation of magmatic-hydrothermal ore deposits. Econ. Geol. 100, 1287–1312.